Winter 11-25-2020

POLEROVIRUS GENOMIC VARIATION AND MECHANISMS OF SILENCING SUPPRESSION BY P0 PROTEIN

Natalie Holste
University of Nebraska-Lincoln, nmholste@gmail.com

POLEROVIRUS GENOMIC VARIATION AND MECHANISMS OF SILENCING SUPPRESSION BY P0 PROTEIN

by

Natalie M. Holste

A THESIS

Presented to the Faculty of

The Graduate College at the University of Nebraska

In Partial Fulfillment of Requirements

For the Degree of Master of Science

Major: Biological Sciences

Under the Supervision of Professor Hernan Garcia-Ruiz

Lincoln, Nebraska

December 2020

POLEROVIRUS GENOMIC VARIATION AND MECHANISMS OF SILENCING SUPPRESSION BY P0 PROTEIN

Natalie M. Holste, M.S.

University of Nebraska, 2020

Advisor: Hernan Garcia-Ruiz

The family Luteoviridae consists of three genera: Luteovirus, Enamovirus, and Polerovirus. The genus Polerovirus contains 32 virus species. All are transmitted by aphids and can infect a wide variety of crops from cereals and wheat to cucurbits and peppers. However, little is known about how this wide range of hosts and vectors developed. In poleroviruses, aphid transmission and virion formation is mediated by the coat protein read-through domain (CPRT) while silencing suppression and phloem limitation is mediated by Protein 0 (P0)—a protein unique to poleroviruses. P0 gives poleroviruses a great advantage amongst plant viruses and diversifies polerovirus species, but the mechanism of suppression is poorly understood. In this thesis, we profiled the genome-wide variability of poleroviruses to understand genome variability and its relation to host adaptation and we experimentally tested P0 to understand the mechanisms of silencing suppression. Results show that P0 and the CPRT are the most variable. P0 and the CPRT also contained the most sites under positive selection, suggesting that these areas provide mutational robustness in an environment that likely includes genetically diverse aphid vectors, host plants, or a combination. P0 was also cloned and tagged for mechanistic analysis. Transient analysis showed P0 is a strong suppressor of transgene silencing. vsiRNA stability, but not biogenesis, was affected

when in the presence of P0. In addition, P0 with AGO 1, 2, 5, 7, and 10 were found to degrade together. Our results provide novel insights on the genome-wide variation across the polerovirus genome and the mechanism of siRNA silencing suppression by polerovirus P0.

ACKNOWLEDGEMENTS

Throughout the creation of this thesis I have received a great deal of support. I want to thank the University of Nebraska-Lincoln, Nebraska Center for Virology, Department of Plant Pathology, and the National Institute of Health for providing the facilities, structure, and funding to foster exceptional research capabilities and developmental growth. I would like to acknowledge my P.I., Dr. Hernan Garcia-Ruiz, for his outstanding understanding of science and his willingness to efficiently teach it to others. I was inspired by all the thought and effort put into managing the lab and its people—Thank you, Dr. Garcia-Ruiz. I want to express my gratitude to my committee members as well. Thank you, Dr. Jean-Jack Riethoven, for your commitment to our lab and my project. I appreciated the outside perspective on my wet-lab project and the bioinformatics advice on my dry-lab project. Thank you, Dr. Amit Mitra for your dedication to students and willingness and understanding throughout my career here at UNL. I greatly value your analogies, stories, and advice from every talk. I also much appreciated our department head, Dr. Loren Giesler's, openness and willingness to communicate and connect with the students.

I would not have been as successful here if it were not for my co-workers. Thank you, Rosalba, for bringing joy everyday with your contagious laugh, silly jokes, and enlightening conversations Thank you, Kathy, for being a guiding light of stability and reliability, but also knowing when to take a much-needed break. I will miss your home-baked desserts! The both of you were pivotal for my achievements here. I could not do it without your help and advice with my projects, presentations, and life-guidance. I can't wait to see where you two go from here! I also want to thank the undergraduate student

workers who made time in lab much easier from experimental help to the wonderful random conversations started.

I have much gratitude for all the well-organized graduate coordinators I have had across the departments, Joel, Jan, Amber, Margaret and Madilyn. I appreciate all the work put in to answering my many questions and requests. I especially would like to thank Margaret and Madilyn for your help when coordinating everything during my Plant Pathology Graduate Student Association (PPGSA) presidency. And to the fellow officers of the PPGSA, thank you so much for your commitment to rebuilding a strong club for the students here with me. The friends made in the department along the way were instrumental to defining my career here. To Asha, thank you for your great advice and resilience to all situations. I admired how strong you are and how easy it seemed for you to stand up for yourself and others. I will miss your presence. To Eddie, thank you for being my role model and student mentor when arriving here. The little time that I got to know you with will positively impact my life forever. Hi Jess, of everything to take away from my time at UNL, you are my favorite. Your friendship impacted my life immensely and I will treasure it always. You are a wonderful human being.

Lastly, I want to recognize my parents, Grandma, my sister, Michelle, and my partner, Mike, for your unwavering belief in me through the years. I am grateful for your love and support and your ability to keep me going. I did it!

LIST OF TABLES

LIST OF FIGURES

Table of Contents

CHAPTER 1

LITERATURE REVIEW

ENCYCLOPEDIA OF VIROLOGY 4TH EDITION

“POLEROVIRUSES (LUTEOVIRIDAE)”

Garcia-Ruiz, H., Holste, N. M., & LaTourrette, K. (2020). Poleroviruses (Luteoviridae). In Reference Module in Life Sciences. Elsevier. https://doi.org/10.1016/b978-0-12-809633-8.21343-5

Introduction

The family Luteoviridae consists exclusively of plant infecting viruses divided into three genera: Luteovirus, Polerovirus, and Enamovirus (Table 1). Luteoviruses diversified into three genera approximately 1,500 years ago in correlation with the expansion of agriculture. Members of the genus Luteovirus (luteoviruses) contain the standard genome of the entire Luteoviridae family: a single, positive single-stranded RNA (ssRNA) encoding the seven proteins P1 through P7 with multiple overlapping open reading frames (ORFs).

Barley yellow dwarf virus (BYDV) is the type species of the genus Luteovirus, which encode a weak silencing suppressor (P4). Members of the genus Polerovirus (poleroviruses) are similar to luteoviruses and contain an additional protein (P0) that is a strong silencing suppressor. Luteoviruses and poleroviruses shared a common ancestor approximately 900 years ago with P0 deriving separately in the polerovirus lineage. The type species of the genus Polerovirus is Potato leafroll virus (PLRV). Pea enation mosaic virus (PEMV) is the type species of the genus Enamovirus (enamoviruses), which encode P0 but not P4. Within the family Luteoviridae, BYDV and PLRV infect important staple crops and cause major economic damage. However, poleroviruses are the most damaging and diverse genus, and have a wide host range.

Poleroviruses have a single, positive ssRNA genome of 5.3-5.7 kb, encapsidated in an icosahedral non-enveloped virion (Figure 1.1). Unique features of poleroviruses include obligate transmission by aphids in a circulative, non-propagative manner, infection restricted to the phloem, and lack of mechanical transmission. Symptoms induced by poleroviruses include stunting, yellowing, a streaking pattern, and stiff leaves. These symptoms are often confused with adverse environmental factors. Most

poleroviruses can be present in seed, tubers, and plant parts used for vegetative propagation. Furthermore, some plant-virus combinations remain asymptomatic. Currently, there are 32 species in the genus Polerovirus infecting both monocots and dicots (Table 1). These include economically important staple crops including maize, wheat, sugarcane, and potato. Poleroviruses with the most economic importance are PLRV, Sugarcane yellow leaf virus, and three beet-infecting poleroviruses.

Table 1. Taxonomic organization of the family Luteoviridae. Species are grouped by genus.

Genus	Species	Abbreviation	Accession number[a]
Luteovirus	*Barley yellow dwarf virus KerII*	BYDV-KerII	NC_021481.1
	Barley yellow dwarf virus KerIII	BYDV-KerIII	KC559092.1
	Barley yellow dwarf virus – MAV	BYDV-MAV	NC_003680.1
	Barley yellow dwarf virus – PAS	BYDV-PAS	NC_002160.2
	Barley yellow dwarf virus – PAV	BYDV-PAV	NC_004750.1
	Bean leafroll virus	BLRV	NC_003369.1
	Nectarine stem pitting-associated virus	NSPaV	NC_027211.1
	Rose spring dwarf-associated virus	RSDaV	NC_010806.1
	Soybean dwarf virus	SbDV	NC_003056.1
Polerovirus	*Beet chlorosis virus*	BChV	NC_002766.1
	Beet mild yellowing virus	BMYV	NC_003491.1
	Beet western yellows virus	BWYV	NC_004756.1
	Carrot red leaf virus	CRLV	NC_006265.1
	Cereal yellow dwarf virus – RPS	CYDV-RPS	NC_002198.2
	Cereal yellow dwarf virus – RPV	CYDV-RPV	NC_004751.1
	Chickpea chlorotic stunt virus	CpCSV	NC_008249.1
	Cotton leafroll dwarf virus	CLRV	NC_014545.1
	Cucurbit aphid-borne yellows virus	CABYV	NC_003688.1
	Maize yellow dwarf virus RMV	MYDV-RMV	NC_021484.1
	Maize yellow mosaic virus	MYMV	KU248489.1
	Melon aphid-borne yellows virus	MABYV	NC_010809.1
	Pepo aphid-borne yellows virus	PABYV	NC_030225.1
	Pepper vein yellows virus	PVYV	NC_015050.1
	Pepper vein yellows virus 5	PVYV-5	NC_036803.1
	Potato leafroll virus	PLRV	NC_001747.1
	Suakwa aphid-borne yellows virus	SABYV	NC_018571.2
	Sugarcane yellow leaf virus	ScYLV	NC_000874.1
	Tobacco vein distorting virus	TVDV	NC_010732.1
	Turnip yellows virus	TuYV	NC_003743.1
Enamovirus	*Alfalfa enamovirus 1*	AEV-1	NC_029993.1
	Citrus vein enation virus	CVEV	NC_021564.1
	Grapevine enamovirus 1	GVEV-1	NC_034836.1
	Pea enation mosaic virus 1	PEMV-1	NC_003629.1
Unassigned	*Barley yellow dwarf virus – GPV*	BYDV-GPV	NC_039035.1
	Barley yellow dwarf virus – SGV	BYDV-SGV	AY541039.1
	Chickpea stunt disease associated virus	CpSDaV	Y11530.1
	Groundnut rosette assistor virus	GRAV	NC_038509.1
	Indonesian soybean dwarf virus	ISDV	
	Sweet potato leaf speckling virus	SPLSV	NC_038510.1
	Tobacco necrotic dwarf virus	TNDV	

[a] Accession numbers in GenBank. Accessions beginning with NC_ are the reference for a particular species.

Polerovirus physical properties

The polerovirus virion has a T3 icosohedral symmetry with an average diameter of 23 nm (Figure 1.1). The capsid is formed by 180 monomers that consist mainly of the coat protein (CP) (approximately 23 kDa) and also contain minor amounts of a readthrough protein (approximately 80 kDa). The readthrough protein substitutes one coat protein monomer when assembling the virion. The ratio of CP to readthrough protein varies from 4:1 to 100:1. The thermal inactivation point is between 50 and 65°C, with a dilution endpoint between 10-3 and 10-4. Polerovirus virions withstand deep-freeze and thaw, and withstand chloroform and detergents. The longevity in sap at 2°C is between 5 and 10 days.

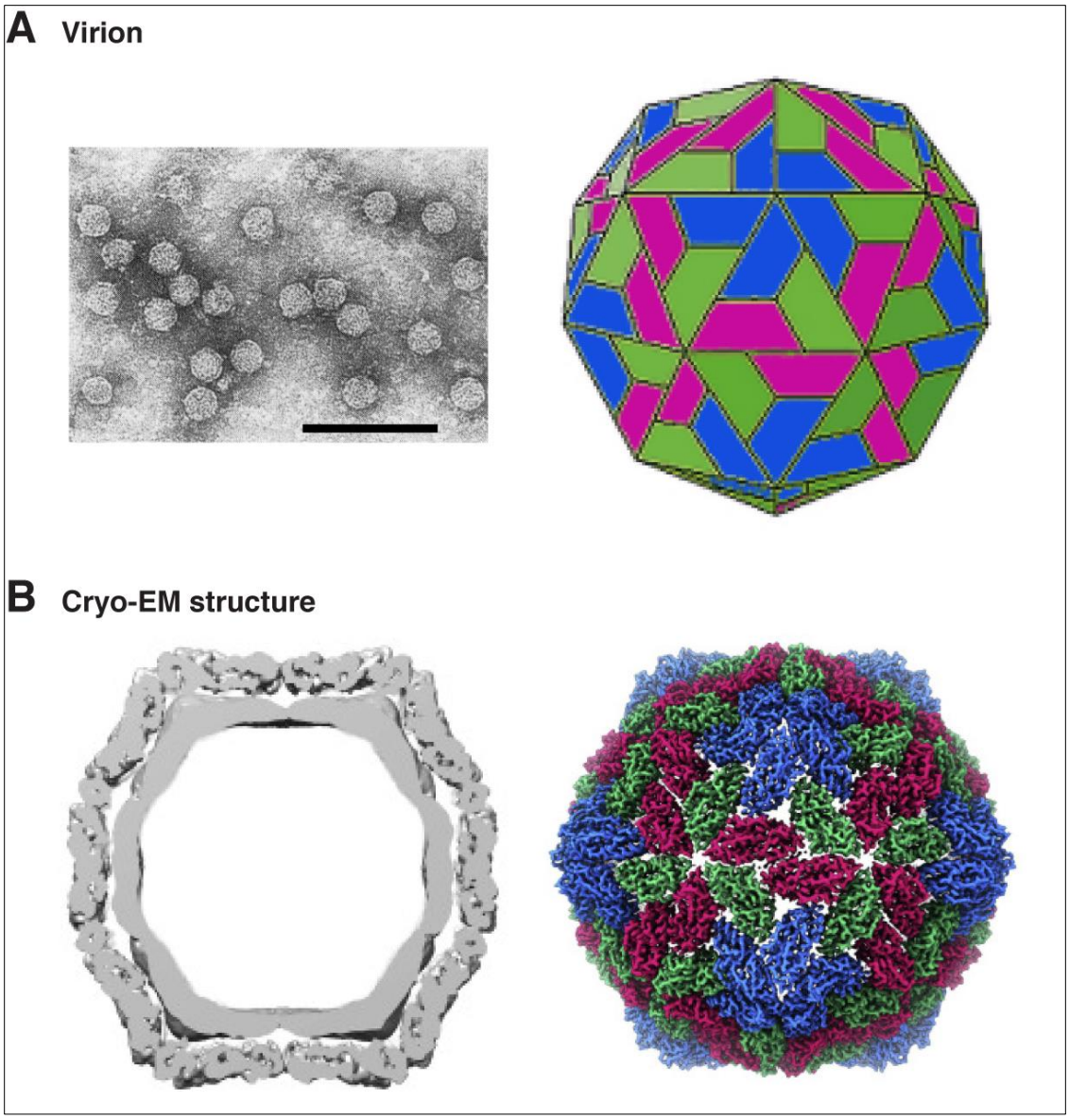

Figure 1.1. Illustration of polerovirus virion structure based on potato leafroll virus (PLRV). A) Transmission electron microscope picture of PLRV virions. The bar represents 100nm. B) The coat protein (CP) creates a virion that with T=3 icosahedral symmetry composed of 180 capsid proteins organized into 60 asymmetric units. colored according to CP quasi-conformers, where subunit A is blue, subunit B is green, and subunit C is red. There is no envelope and the diameter averages 23 nm. C) Cryo-electron microscopy of PLRV-like particles. Section of representative density and molecular model, slice through unsharpened maps, depicting density for packaged RNA and/or disordered R domain. D) cryo-EM maps of whole virus capsid. Structure refinement was carried out with icosahedral symmetry imposed, yielding density maps at a resolution of 3.4 Å. Reproduced with permission from Byrne, M.J., et. al. 2019.

Polerovirus genome organization and gene expression

The polerovirus genome consists of a single, positive-strand ssRNA encoding P0 through P7 organized in overlapping ORFs (Figure 1.2A). The 5'-end is protected by the genome-linked protein VPg. The 3'-end contains an -OH group and lacks a poly-A tail. Two sub-genomic RNAs are formed during replication. Translation of polerovirus proteins involves a combination of strategies: leaky scanning, internal ribosomal entry, frameshift, and ribosomal read-through (Figure 1.2B). Additionally, VPg is released from protein P1 by protease processing.

Proteins P0 and P1 are translated from the genomic RNA using leaky scanning and alternate translation initiation codons (Figure 1.2B). P1 can be expressed either individually or fused with P2. When P1 is expressed by itself, it contains two putative domains: VPg and a protease that releases VPg. A ribosomal frameshift produces a P1-P2 fusion protein that generates the RNA-dependent RNA polymerase (RdRp) responsible for viral RNA replication and sub-genomic RNA synthesis. P2 is never expressed by itself. Replication associated protein 1 (Rap1) is translated from genomic RNA through an internal ribosome entry site (IRES).

Protein 3a and the movement protein (MP, P4) are translated by leaky scanning from sub-genomic RNA1 and both are involved in virus movement along with the CP. A ribosomal read-through is required for the translation of the CP read-through (P3-P5), which is less abundant than the CP (P3). An amber stop codon (UAG) separates these ORFs in sub-genomic RNA1 (Figure 1.2B). The CP read-through is not necessary for virion formation, but it is essential for aphid transmission and virus movement in plants. The N-terminal half of the CP read-through determines vector specificity by regulating the efficiency of virus movement through the salivary tissues

and gut. Accordingly, mutants lacking the CP read-through accumulate to low levels and are not transmitted by vectors. The C terminal half of the CP read-through is involved in efficient virus movement, tissue tropism, and symptom development in plants.

Several proteins in the genome are currently not well understood. P3a is newly discovered part of the genome. It sits directly upstream of the CP ORF (P3) and is translated by a non-AUG start codon. P3a is required for long-distance movement of poleroviruses. Proteins P6 and P7 are translated by leaky scanning from sub-genomic RNA2. P7 has nucleic acid binding properties. However, the biological role of P6 and P7 remains to be determined.

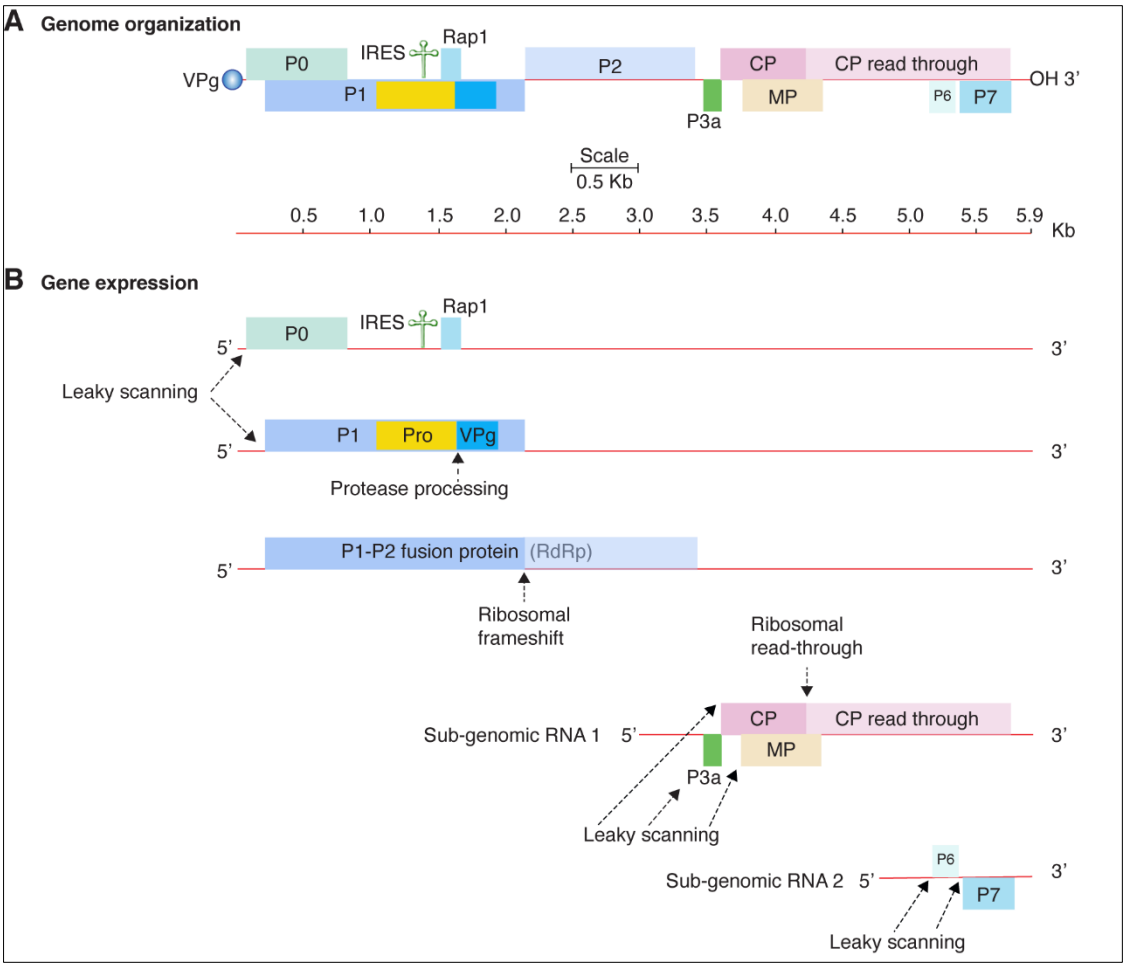

Figure 1.2. Schematic representation of polerovirus genome organization and gene expression. Single lines represent non-coding regions and labeled boxes represent cistrons. Sub-genomic RNAs, their formation and proteins translated from them are indicated. A) Generalized polerovirus genome organization. Coordinates are based on Potato leafroll virus accession number KY856831. B) Polerovirus gene expression strategies include formation of sub-genomic RNAs, translation by IRES-mediated internal initiation, leaky scanning, ribosomal frameshift, and ribosomal read-through. Protein 1 is processed into mature VPg by proteolysis. Pro: Putative protease. VPg: Viral protein genome-linked. RdRp: RNA-dependent RNA polymerase. Rap1: Replication associated protein. CP: Capsid protein, major and minor. MP: Putative movement protein. p3a: Protein essential for systemic virus movement. IRES: Internal ribosomal entry site.

Polerovirus phylogenetic diversity

The evolutionary relationship and phylogenetic diversity of poleroviruses is just beginning to be elucidated. Published studies used the CP and read-through domains

based on the assumption that they are highly conserved (Figure 1.3). Based on the CP (Figure 1.3A), PLRV is an out-group, while Pepper yellow leaf curl virus (PYLCV), Pepper vein yellows virus (PeVYV), and Pepper yellows virus (PepYV) clustered on the same branch, and probably evolved from TVDV. However, the N-terminus of the CP read-through (Figure 1.3B) separates Tobacco vein-distorting virus (TVDV) and places Cucurbit aphid-borne yellows virus (CABYV) close to pepper-infecting poleroviruses. In contrast, the C-terminus of the CP read-through (Figure 1.3C) separates pepper-infecting poleroviruses and place TVDV close to PYLCV. Differences in the arrangements of poleroviruses based on CP, N or C terminal parts of the CP read-through suggest that RNA recombination occurs frequently and is an important contributor to the evolution of poleroviruses.

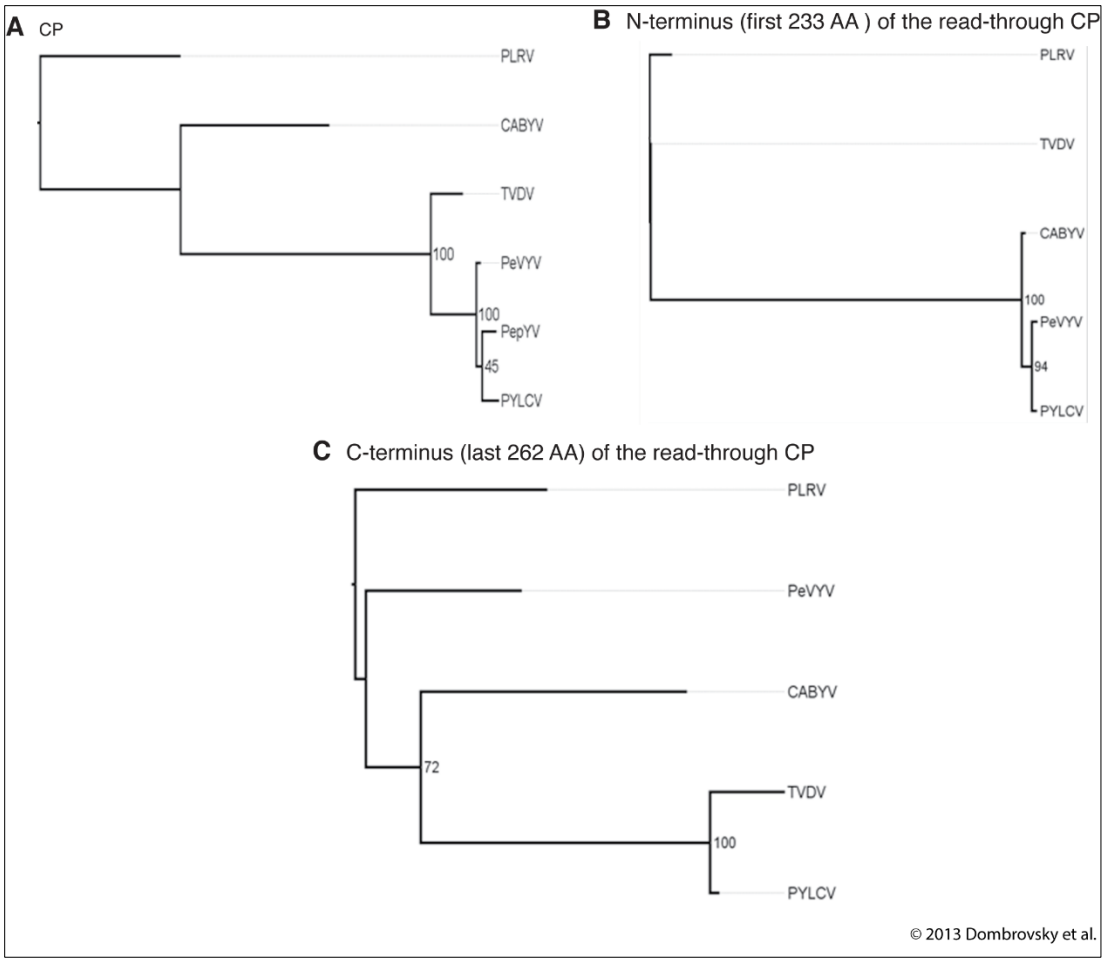

Figure 1.3. Phylogenetic analysis of selected poleroviruses based on the following proteins: (A) CP (ORF3), (B) the N-terminus of the RTD (ORF5, first 233aa) (C) the C-terminus of the RTD (ORF5, last 262aa) of Potato leaf curl virus [PLRV (Y07496)], Tobacco vein-distorting virus [TVDV (EF529624)], Cucurbit aphid-borne yellows virus [CABYV (X76931)], Pepper vein yellows virus [PeVYV (AB5948280)], Pepper yellow leaf curl virus [PYLCV (HM439608)], and Pepper yellows virus [(PepYV) FN600344].

Polerovirus transmission

Polerovirus species have evolved to be efficiently transmitted by particular aphid species. PLRV is efficiently transmitted by Myzus persicae, while maize poleroviruses are efficiently transmitted by the corn leaf aphid (Rhopalosiphum maidis). Other aphids that vector poleroviruses include R. padi, Stiobion avenae, and Aphis gossypi. Aphids vector poleroviruses in a circulative, non-propagative manner.

The cycle begins when an aphid feeds on a polerovirus-infected plant. The virus first will reach the salivary glands of the aphid. It has been found that the readthrough domain is not required for the virion to cross the salivary gland, but it does improve the success of the transport. If the species is from a yellow dwarf lineage, the virion then moves through the hindgut. If the species mainly uses dicots as their host, such as PLRV or Beet western yellows virus (BWYV), the virion instead moves through the midgut. Once inside the gut, the virus normally moves between the cytoplasm and the epithelial cells. It then fuses with the plasmalemma and is released between the basal lamina and the membrane. Aphids can then release the virion into the phloem parenchyma and/or the companion cells to initiate local infection. Cell-to-cell and systemic infection may occur and require the combined activity of the movement protein, capsid protein, capsid protein read-through, and P0. Phloem-limited viruses cannot normally be mechanically transmitted. However, using particle bombardment, infection has been achieved with PLRV and BWYV. The high number of aphid vectors allows poleroviruses to infect a wide range of hosts.

Potatoes, sugarcane, and beets are important species infected by poleroviruses. These all propagate in a vegetative manner. Poleroviruses can spread through infected contaminated plants parts used for propagation, such as tubers and sugarcane cuttings.

Virus-virus interactions

Co-infections of PLRV with Potato virus X (PVX) (Potexvirus) or Potato virus Y (PVY) (Potyvirus) result in an enhancement in symptom severity and yield loss. Similarly, co-infection of Brassica yellows virus (BrYV) (unassigned Polerovirus) and Pea enation mosaic virus 2 (PEMV-2) (Umbravirus) results in similar synergism. PEMV 2 is an umbravirus that accompanies PEMV as a satellite virus. PEMV-2 can only infect

plants when a member of the Luteoviridae is present. Co-infection of BrYV and PEMV-2 results in higher accumulation of BrYV, more severe symptoms, and the acquisition of mechanical transmission.

Co-infection of BWYV and the potyvirus Beet mosaic virus (BtMV) causes faster systemic virus movement and earlier, more severe symptoms. The combination of the polerovirus and the potyvirus disrupts photosynthesis and vascular transport, and both viruses accumulate to high levels when co-infected. Experimentally, the potyvirus helper-component proteinase (HC-Pro), a strong silencing suppressor, increased the accumulation of PLRV. It also allowed the virus to spread into mesophyll cells.

Maize lethal necrosis is a re-emerging disease of current epidemic proportions in sub-Saharan Africa. Maize lethal necrosis disease was discovered in 1976 in Nebraska and Kansas, USA. It was caused by Maize chlorotic mottle virus (MCMV) in combination with a potyvirus, Sugarcane mosaic virus (SCMV). Several recent studies have found poleroviruses in maize in combination with MCMV, SCMV, or both. The poleroviruses detected include the Maize yellow dwarf virus-RMV (MaYMV), Maize yellow mosaic virus (MaYMV), and Barley virus G (BVG). However, MYDV-RMV was the most common. Plants with a combination of a polerovirus, SCMV, and MCMV have atypical symptoms. These and other observations suggest that poleroviruses, in combination with MCMV, could also cause maize lethal necrosis disease.

Silencing suppression by poleroviruses

In plants, gene silencing is an essential component of antiviral defense. Virus infection induces antiviral gene silencing. Argonaute (AGO) proteins are the catalytic components of the RNA-induced silencing complex (RISC) and associate with cellular or virus-derived small interfering RNAs (siRNA). Binary complexes formed between

argonaute proteins and siRNAs specifically target RNA, including viral RNA, complementary to the siRNA. They have also been implicated in cell-to-cell and systemic movement of gene silencing signals. This results in amplification of gene silencing in areas beyond the initial activation site, thereby conferring virus immunity.

In order to establish infection and move within plants, viruses encode specialized proteins that suppress gene silencing. In poleroviruses, P0 is a silencing suppressor. P0 silencing suppression activity has been demonstrated for 10 of the 32 poleroviruses (Table 1). For Beet chlorosis virus (BChV), and some strains of Beet mild yellowing virus (BMYV), no silencing suppression activity was found for P0. For all other poleroviruses, no information is available or the suppression activity of P0 has not been determined. In standard experimental assays, for some poleroviruses, P0 suppresses either local or both local and systemic gene silencing.

P0 suppresses gene silencing by targeting argonaute 1 (AGO1) protein for degradation by ubiquitination. Through the F-box-like motif, P0 interacts with the DUF1785 motif in AGO1 to mark it for degradation. In Arabidopsis thaliana, the P0 F-box-like motif interacts with the F-box of the S phase kinase-associated protein 1 (SKP1) and with the ASK1 and ASK2 orthologues. AGO1 is the primary interaction partner of microRNAs and is a crucial for normal plant development. Thus, symptoms induced by polerovirus infection are in part due to the effect on AGO1, and potentially other AGO proteins being tagged for degraded by P0 which in turn affects normal plant development.

Potato leafroll virus

PLRV is the first polerovirus discovered, one of the most damaging poleroviruses worldwide, and the most damaging potato virus. It is highly prevalent and has been

found on every continent except Antarctica. PLRV was first detected in the 1770's, causes 50-60% yield loss, and costs the United States 100 million-dollars yearly. PLRV is transmitted by infected tubers and by aphids. When the virus is transmitted by aphids, symptoms begin in young, top leaves that roll and turn pale. When grown from an infected tuber, the plants may be pale or dwarfed, and the leaves may be upright, rolled, yellow, or brittle (Figure 1.4A). However, the appearance of water-soaked leaves is usually the first symptom. In the stem and the tuber sieve tubes, abnormal amounts of callose accumulates. The carbohydrates in the leaves reach high levels causing the phloem transport to be impaired, which results in tuber reduction. This could occur because photo-assimilation is reduced, sucrose is unable to enter the phloem, or a combination of the two. These factors result in leaves with an upright and rolled appearance. In some cultivars, the margins of the leaves may turn purple or red and develop necrosis in later stages. This necrosis starts in the phloem of the petioles and stems.

Sugarcane yellow leaf virus

Worldwide, damage by poleroviruses in sugarcane is a close second to PLRV. ScYLV is a good representation of the yellow leaf or yellow dwarf viruses amongst poleroviruses. ScYLV was first discovered in Hawaii in 1989 and is distributed world-wide. Currently, it is primarily detected in South America, Asia, and the Pacific islands. ScYLV affects sugarcane production in over 90 countries, which grow sugarcane for sugar, biofuel, and fibers. Crops affected by ScYLV have losses that reach up to 43%, and it is spread by infected seed canes and aphids. ScYLV infection reduces the cane thickness, the number of canes produced, and the rate of photosynthesis in the plant. It causes yellowing at the midrib (Figure 1.4B), and, at 6 to 8 months, the yellowing

spreads laterally to the leaf lamina and causes necrosis at the tip. Because of the short internode spacing, this causes the plant to be dwarfed. Interestingly, when co-infected with a certain bacterium, Leifsonia xyli sub species xyli, it increases the severity of the disease. Even when the virus is latent in the plant, the yield is decreased, especially in non-resistant varieties. Unfortunately, all yellow leaf viruses are hard to distinguish from normal environmental damage.

Beet poleroviruses

The three main poleroviruses infecting beet are BWYV, BMYV, and BChV (Table 1). Most of the strains are different isolates of BWYV originating from Europe. Within the last decade, the virus has spread to Australia and resulted in a 26% yield loss in pluses, canola, and various vegetables. In canola, 59% of the 65% yield loss was due to BWYV alone. BMYV is also known to result in about 22% crop loss if it appears in June. However, it has been found that these viruses have a much broader host range within the whole Amaranthacae family, temperate legume crops, and brassicas. They also widely infect the weeds that grow around these crops. Of the beet-infecting poleroviruses, BChV has a smaller a host range because it only infects sugar beets. These persistent viruses are transmitted by a wide variety of aphids, with the highest being the genus Myzus. Normally, sugar beets are durable crops that are tolerant to drought and can withstand intense wilting with no yield loss. However, poleroviruses cause stunting, chlorosis, rolling leaves, stiff followed by brittle leaves, and yellowing in the veins (Figure 1.4C). Some leaves may turn orange rather than the typical yellow, which starts at the tip of the leaves. Beet-infecting poleroviruses remain problematic because of their impacts on crops, wide host range, and difficulty to diagnosis.

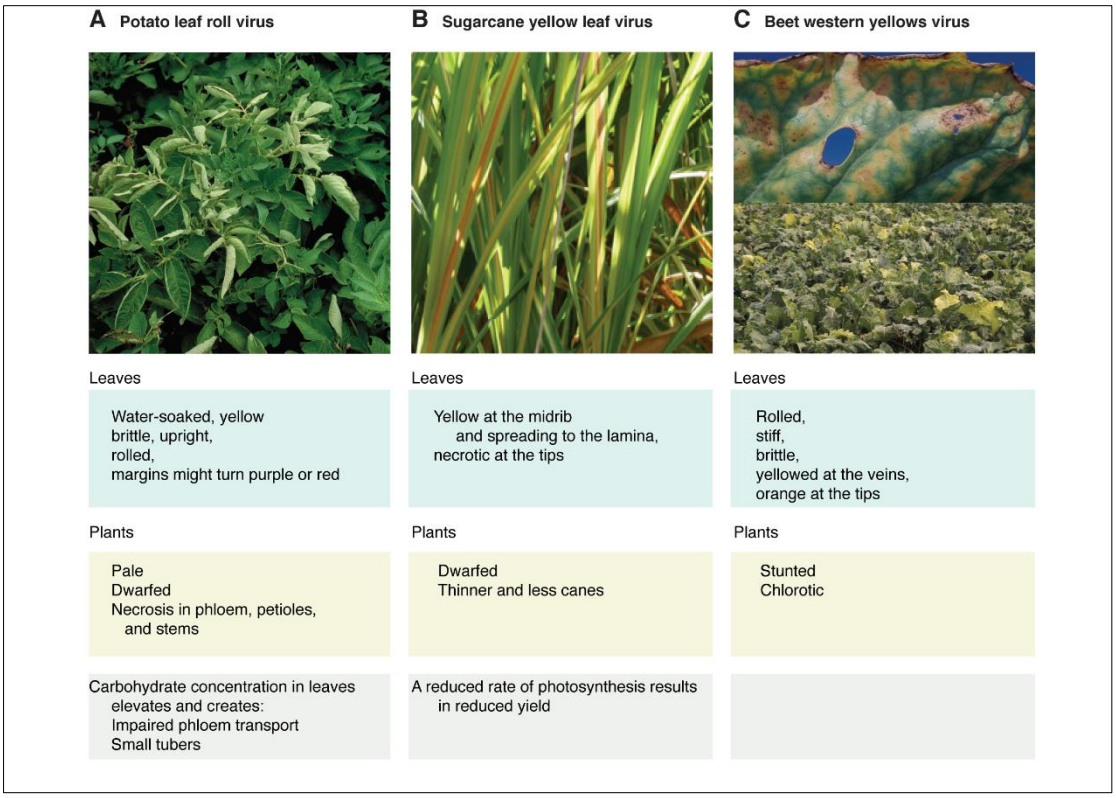

Figure 1.4. Representative symptoms, in leaves and whole plants, caused by the top three poleroviruses. Other features of the symptoms are described below the images. A) Symptoms caused by Potato leafroll virus in potato plants and leaves. Reproduced with permission from Jack Kelly Clark, University of California Statewide IPM Program. B) Symptoms caused by Sugarcane yellow leaf virus in sugarcane. Reproduced with permission from CIRAD: The French Agricultural Research Organization working for the sustainable development of tropical and Mediterranean regions. C) Symptoms caused by Beet western yellows virus is sugar beet. Reproduced with permission from G.J. Holmes, California Polytechnic State University at San Luis Obispo.

Diagnosis

There are several methods of detecting poleroviruses. The first test designed was the Ingel-Lange test. This test stained callose with a resorcin blue dye in the tubers of a potato infected with PLRV. Currently, poleroviruses are detected using a variety of RNA-based and protein-based approaches. Protein-based approaches use antibodies that recognize the capsid protein. The most common protein-based approach is

enzyme-linked immunosorbent assay (ELISA). A variation is the double antibody sandwich ELISA. Other protein-based approaches include immune-electron microscopy, immune-electrophoresis, and double diffusion agar tests.

RNA-based approaches include reverse-transcription polymerase chain reaction (RT-PCR), deep sequencing of the siRNAs, and high-throughput sequencing of transcript RNA. There are universal polerovirus primers for detection by RT-PCR. Universal primers Pol-G-F and Pol-G-R amplify a 1.4 kb PCR product spanning part of the RdRp gene, the intergenic region, and the complete CP gene. Additionally, northern blotting may be used to detect genomic and sub-genomic RNAs.

Electron microscopy is commonly used to visually detect poleroviruses. Using the transmission electron microscope, Cereal yellow dwarf virus (CYDV), BWYV, PLRV, and CABYV have been observed being transported through the gut and epithelial cells into the aphid. Electron microscopy was also used to track the readthrough domain to determine its role inside the aphid.

Disease management

Polerovirus resistant plants are not common. In crops of economic importance, there are no polerovirus-resistant varieties. Varieties that do exist are only resistant to one or a few strains of the virus. Because resistant cultivars impose selection pressure and viruses mutate quickly, viruses break genetic resistance within a few years.

Since poleroviruses are vectored by aphids, physical barriers have been implemented to prevent polerovirus spread. Plastic reflective mulch can be placed around the crops. UV wavelengths will be reflected, thus repelling the aphids. Floating row covers with a fine mesh can also physically block the aphids from reaching the plant. Topical approaches include mineral oil and aphicides. Mineral oil can be applied

to crops to smother aphids. Aphicides can be used on plants similar to chemical pesticides.

Carefully planned planting can reduce virus transmission by aphids. Planting when aphids are low, like after a short rain season, could potentially reduce the number of aphids in the field. This strategy can then be combined with timed pesticide use. Government restricted closed seasons for planting certain crops will also reduce polerovirus transmission. Several countries already restrict crop planting during certain times, but the approach could be further expanded around the globe. Farmers should also practice good crop rotation and diversification. A maize and soybean rotation will likely have different aphid vectors, so there is a decreased likelihood of continual crop infection. A less practiced method is to control the weeds in the field. Weeds that are not removed between crop planting could still be infected, thus leading to crop infection in the next season. It is also good practice to burn any infected plant material because it is the only surefire method to destroy the virus. This method also eliminates the possibility aphids may feed on infected plant material and spread the infection to healthy plants. Aphids are attracted to bare soil, so farmers should work to plant crops closer, include cover crops, and have untilled soil. Preventative measures provide options to limit poleroviruses exposure, but the possibility of resistant plants remains the only option to fight infection directly.

CHAPTER 2

GENOMIC VARIATION ACROSS POLEROVIRUS SPECIES

LaTourette, K.*, Holste, N.*, and Garcia-Ruiz, H.

* These authors contributed equally to this work

INTRODUCTION

Luteoviridae encompasses three families of plant viruses: luteoviruses, poleroviruses, and enamoviruses. This family consists of positive, single-stranded RNA viruses ranging from 5.5 to 6 kb of overlapping reading frames (Krueger, et. al., 2013). All three luteovirids contain two conserved regions: a capsid protein (CP) at protein (P)3 and a coat protein readthrough domain (CPRT) from P3 through P5 conferring aphid transmission (Krueger, et. al., 2013). Luteoviruses and poleroviruses contain a P3a for long distance movement, P6 of unknown function, and a phloem-restricting, cell-to-cell movement protein (MP) at P4. Enamoviruses lack MP allowing enamovirus mechanical transmission. Upstream of CP, poleroviruses and enamoviruses have high similarities with Sobemoviruses rather than luteoviruses (Krueger, et. al., 2013). Poleroviruses and enamoviruses contain the RNA-dependent RNA polymerase (RdRp) at P1 through P2, a VPg cap encoded within P2, and an RNA silencing suppressor at P0. A P7 has been found in poleroviruses and has no assigned function (Pagán & Holmes, 2010).

The diversity in the Luteoviridae arises from a splitting event 900 years ago that formed luteoviruses and poleroviruses (Fusaro et al., 2017; Krueger et al., 2013). This diversification, similar to the evolution of other plant viruses, is likely correlated with agricultural expansion (Pagán and Holmes, 2010). This divergence resulted in the development of a key component in poleroviruses, the RNA silencing suppressor protein (Kruger et al., 2013). P0 is one of the most diverse proteins of the polerovirus genome along with the coat protein. Diversity in viruses typically correlates with multi functionality (Ritz, et. al, 2013). In addition to the originally known function of P0, VPg, and the coat protein, it has been shown that all of these proteins contribute to vector specificity as well (Patton et al., 2020).

Poleroviruses are a diverse genus of viruses with a broad host range (Garcia et al. 2020). There are 32 poleroviruses distributed worldwide that cause damaging diseases in a wide variety of plants including potato, sugarcane, maize, and beets (Garcia-Ruiz, et. al., 2020). The type species for poleroviruses is Potato leafroll virus, which is the most damaging potato virus and one of the most damaging poleroviruses (Garcia et al. 2020). Poleroviruses are obligatorily transmitted by aphids and infection is limited to the phloem. Symptoms generally include stunting, yellowing, and leaf malformations (Garcia-Ruiz, et. al., 2020).

The polerovirus genome forms two sub-genomic RNAs during replication, which require several different translation methods (Garcia et al. 2020). By containing alternative initiation codons within P0, leaky scanning is used to code for P1. P1 can be expressed alone or in conjunction with P2 when a ribosomal frameshift occurs (Nixon et al., 2002; Prüfer et al., 1992). The VPg is created when the P1-encoded protease releases VPg from the intermediate (Toba, et. al., 2006). Leaky scanning is utilized to create P3, P3a, and P4 as well. P3 and P5 are both needed to create the T=3 icosahedral virion while P5 is also important for vector transmission and virus movement. (Peter et al. 2008) P3 is the major protein and is coded alone a higher percentage of the time. To encode P5, the ribosomes must skip over the CP stop codon and continue through the read-through domain that synthesizes the P3-P5 coat protein. This read-through domain is then incorporated into the 23-25 nm virion (Xu et al., 2018, Garcia et al., 2020).

Viruses must retain flexibility in their genomes in order to adapt to different hosts and vectors (Nigam et al., 2019, Nigam et al., 2020). Several methods have been

utilized to determine areas of hypervariability including using non-synonymous to synonymous ratios, genome-wide analysis of Single Nucleotide Polymorphisms (SNPs), and calculating nucleotide diversity (Pi), and protein disorder (Nigam et al., 2019; Rodamilans et al., 2018). In poleroviruses specifically, a brief analysis of 9 polerovirus genomes showed that SNPs were concentrated at the 5' and 3' cistrons (Huang et al., 2005). However, SNPs are significantly lower between P2 through P4 showing that the RNA-dependent-RNA-polymerase is conserved (Huang et al., 2005). Another study showed Barley yellow dwarf virus (BYDV) isolates closely related to BYDV polerovirus isolates harbored two hypervariable areas within the coat protein (CP) (Liu et al., 2007).

It has also been suggested that poleroviruses species have high recombination rates, contributing to new species and species evolution (Dombrovsky et al., 2013). Recombination between viruses can occur when both viruses infect a host at the same time, which can result in different genomic sections having different phylogenetic histories (Moonan et al. 2000). Several recombination mechanisms in poleroviruses have been proposed. One option is that recombination in viruses occurs at specific areas of the genome called recombination breakpoints. For poleroviruses, potential recombination breakpoints are located between the RdRps and the CP region in the non-coding internal region (IR) and between RdRp ORF1 and ORF2 (Dombrovsky et al., 2013, Pagán and Holmes, 2010, Kwak et al., 2018). This area correlates with the start sites of subgenomic RNA-1 synthesis (Miller et al. 1995).

The areas of variation and conservation across the Polerovirus genus are poorly understood. Several proteins have been reported as multifunctional proteins within the genus. Multifunctional proteins are typically highly disordered and hypervariable. A

disordered protein is identified as protein with the ability to fold into varying shapes to adapt to varying functions. (Rodamilans et al., 2018) These proteins confer a wide range of host plants and vectors and have not been characterized at a full-genome level. Multifunctionality and high disorder in proteins create a wealth of function in small viruses with low numbers of proteins and are often mutationally robust. An understanding of where these areas lie will elucidate understandings of polerovirus evolution, protein functions, and host adaptation.

Here, we used SNPs, nucleotide diversity, selection analyses and disorder to map polerovirus genomic variation patterns. Our study showed that poleroviruses contain hypervariable areas at P0 and the CPRT while P2 and the CP are the most genetically stable cistrons, with the exception. These hypervariable areas are conserved across different polerovirus species. P0 and the CPRT also had the highest number of sites under positive and negative selection. The CPRT showed to be highly disordered, which coupled with its hypervariability and positive selection sites, suggests it is important for host adaptation. Ultimately, our findings outline the areas to target for future studies involving universal polerovirus diagnostic tests, breeding and creating resistant plants, and determining areas of host adaptation.

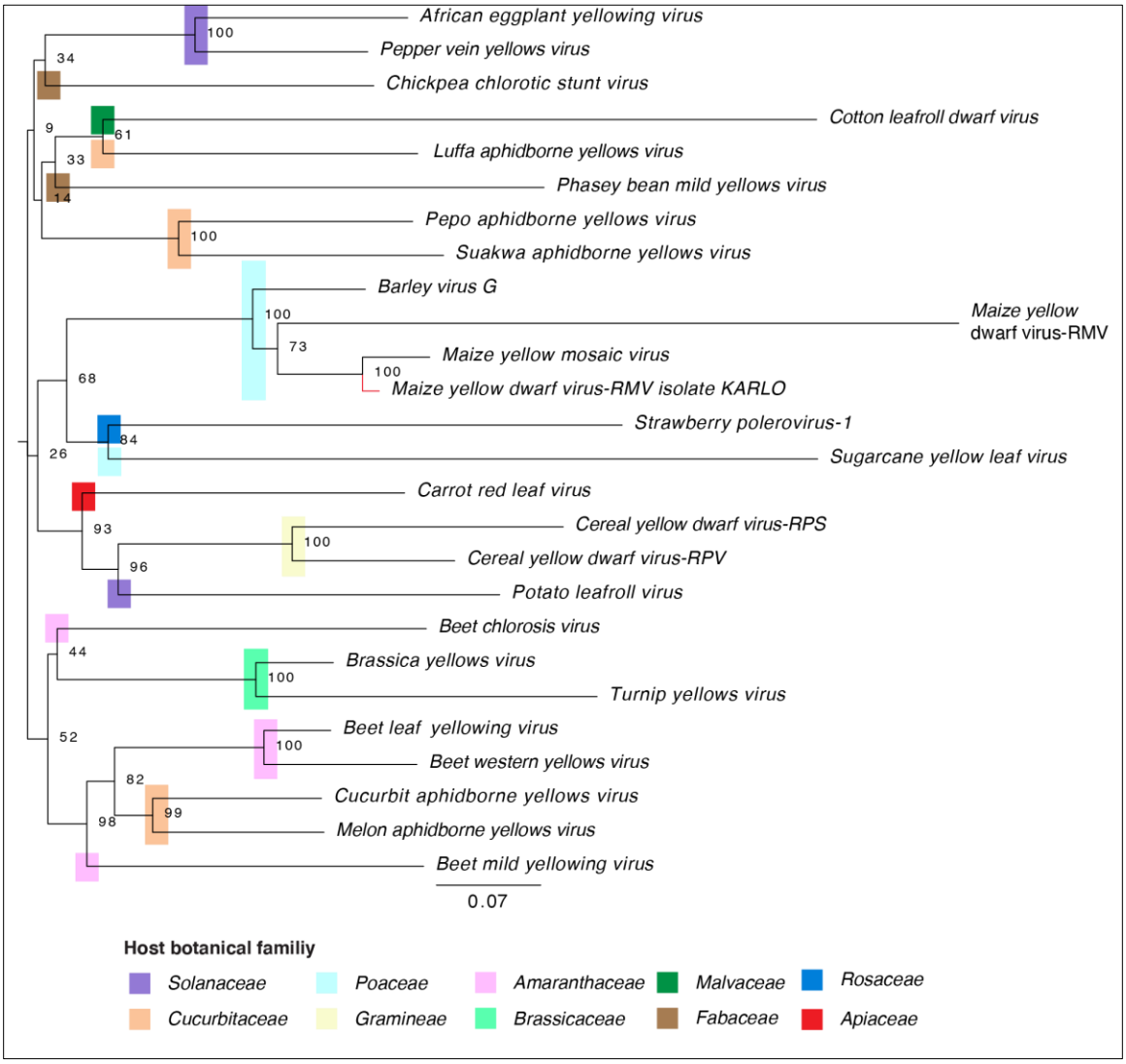

Figure 2.1. Polerovirus phylogeny based on consensus nucleotide sequences. Neighbor-joining tree with bootstrap values (100) generated using MAFFT. Family of the host is marked by colored bars. KARLO isolate is marked in red.

RESULTS

Polerovirus phylogeny and botanical family of their hosts

To determine the genetic relationship across all polerovirus species, a novel, nucleotide-based phylogenetic tree was created. The 26 poleroviruses formed a monophyletic group with 7 different viral clusters. These clusters were based on the

botanical family of their host, indicated by separate colors (Figure 2.1). This groups included hosts from Solanaceae, Cucurbitaceae, Poaceae, Gramineae, Amaranthaceae, and Brassicaceae. Each host family formed viral cluster except for Cucurbitaceae which formed two. Chickpea chlorotic stunt virus (CCSV), Cotton leafroll dwarf virus (CLRDV), Phasey bean mild yellows virus (PBMYV), Strawberry polerovirus-1 (SPV-1), and Potato leafroll virus (PLRV) did not fall into a host cluster. The Maize yellow dwarf virus-RMV (MYDV-RMV) isolate KARLO formed a monophyletic clade with Maize yellow mosaic virus (MaYMV). In Wamaitha et al., the KARLO isolate was later identified as MYDV-RMV or a new species (2018). With new sequence data since that publication, we have concluded that the KARLO isolate is most closely related to MaYMV rather than MYDV. This suggests viruses infecting similar hosts are exposed to similar selection pressures and thus share similarity at a genomic level.

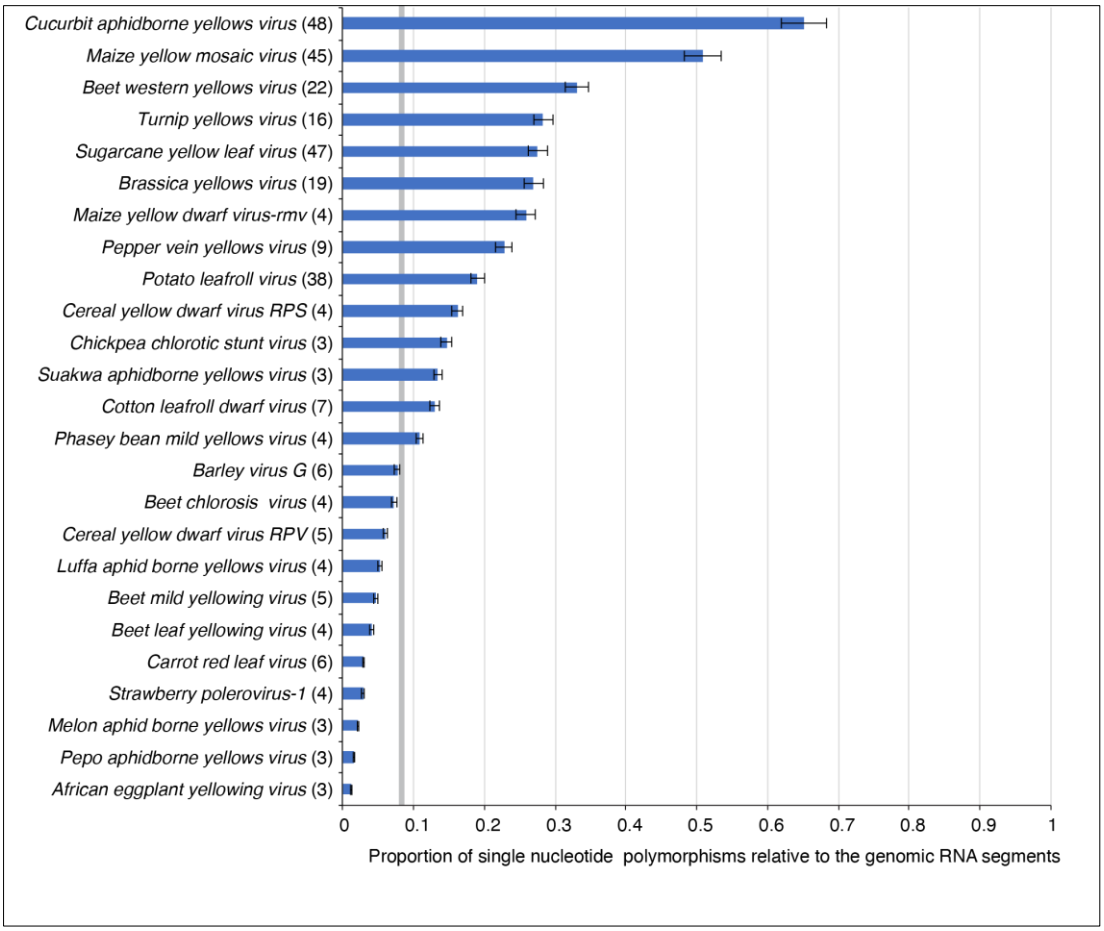

Figure 2.2. Single Nucleotide Polymorphisms in polerovirus RNA. Bars represent the genomic variation index, expressed as the proportion of polymorphic sites relative to the length of the segment. For each species, the number of nucleotide accessions for each segment are indicated in parenthesis. The gray vertical line represents the mean and a 99% confidence interval (p-value < 0.01).

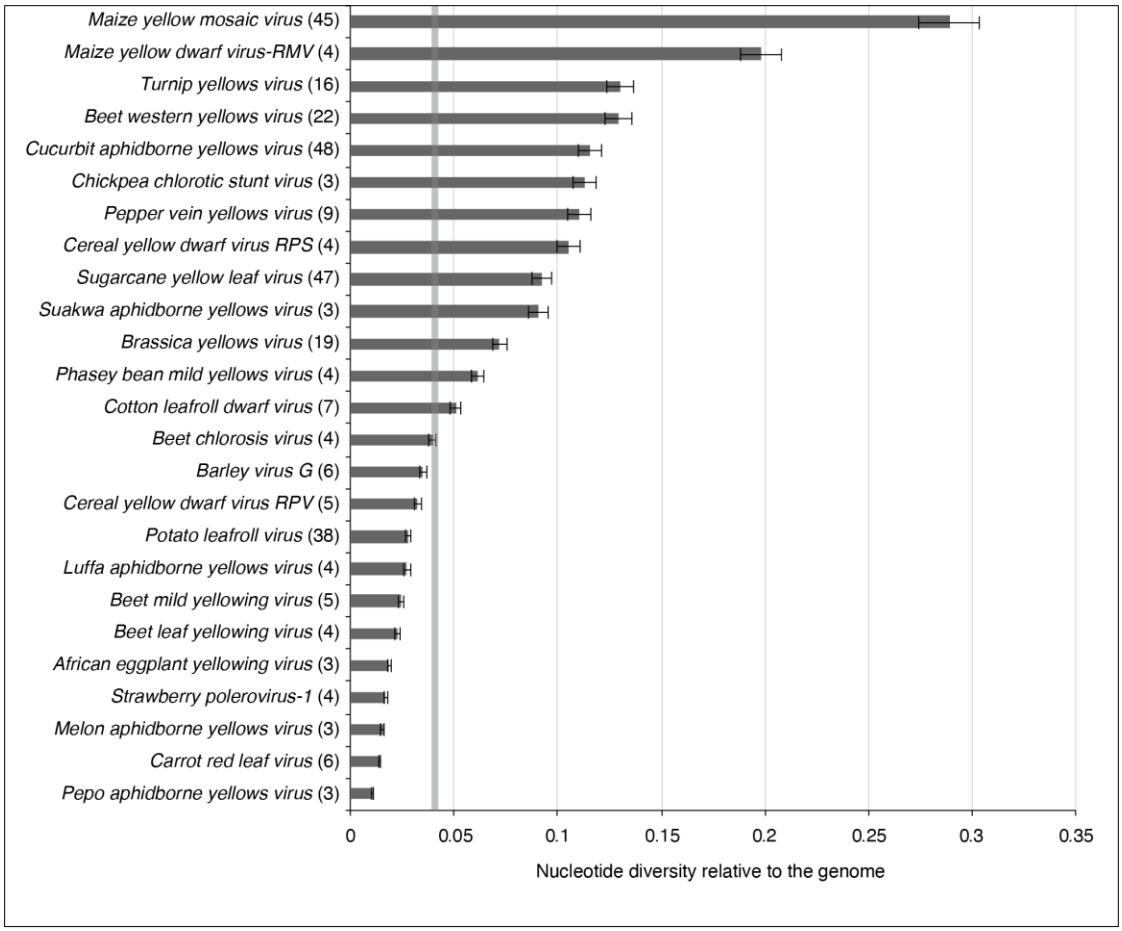

Figure 2.3. Nucleotide diversity in poleroviruses. Bars represent the proportion of variable positions with respect to the length of the genomic segment normalized to the number of accessions. For each species, the number of nucleotide accessions for each segment are indicated in parenthesis. The gray vertical line represents the mean and a 99% confidence interval (p-value < 0.01).

Poleroviruses nucleotide variation

Nucleotide variation was measured for each polerovirus species using SNPs and Pi. Only polerovirus species with at least three different accessions were used. 14 of the 25 poleroviruses had a genomic variation index of at least 10%. Cucurbit aphid-borne yellows virus (CABYV), MaYMV, and Beet western yellows virus (BWYV) poleroviruses have the highest variation with at least 30% of their genome being polymorphic (Figure 2.2). To account for the differences in the number of accessions, variation was

measured in parallel using Pi. Pi contains a parameter which normalizes the number of accessions. (Nigam et al., 2019) Based on Pi, MaYMV, MYDV-RMV, Turnip yellows virus (TuYV), BWYV, and CABYV had the highest variation (Figure 2.3). The five most variable poleroviruses based on the Pi analysis (MaYMV, MYDV-RMV, TuYV, BWYV, and CABYV) and the type species, Potato leafroll virus (PLRV), were selected for all further downstream analyses.

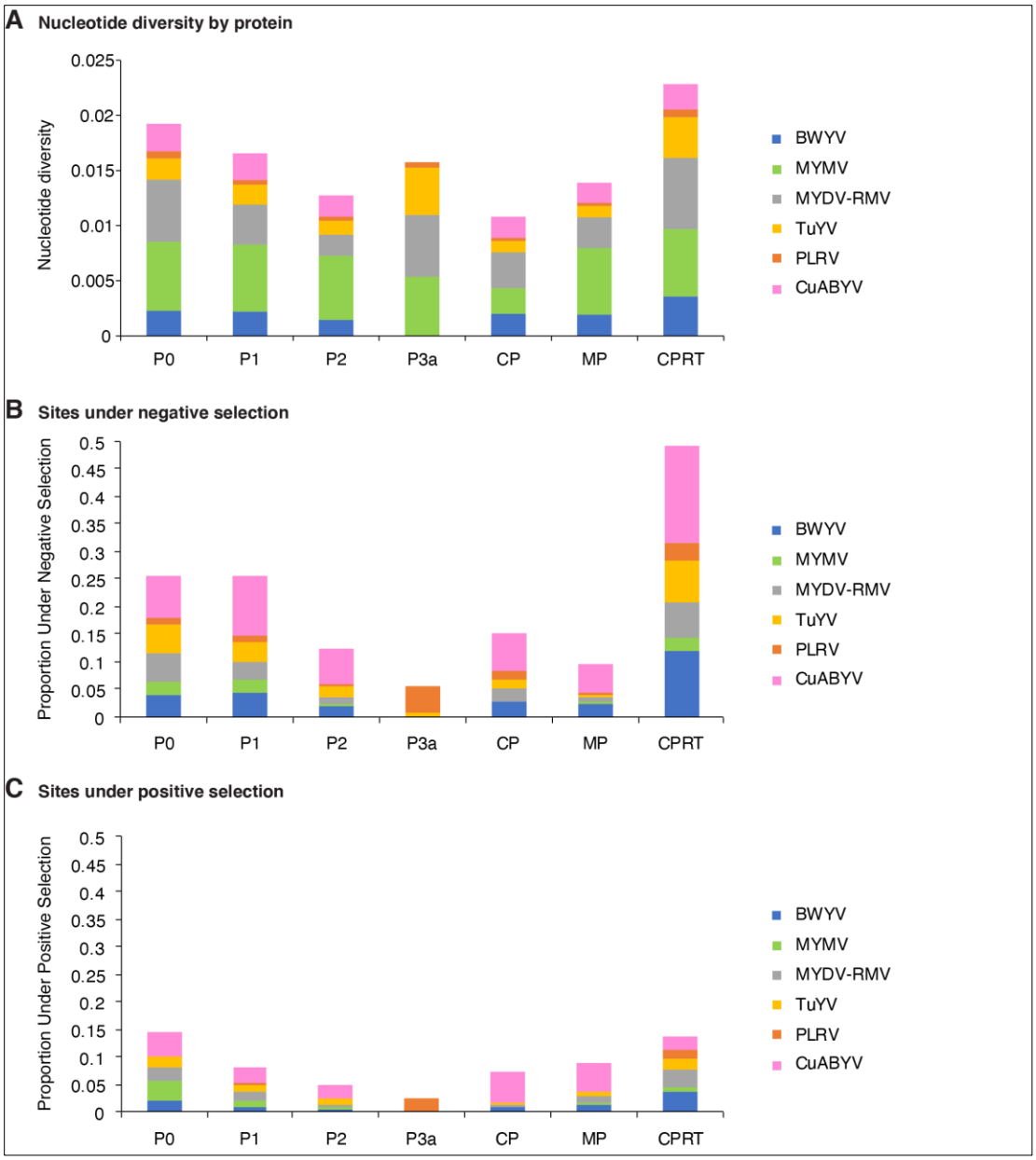

Figure 2.4. Nucleotide diversity, positive, and negative selection in the top 5 most variable poleroviruses and type species. (A) Cumulative nucleotide diversity normalized to the length of the genomic RNA segment. (B) Frequency of the sites under negative selection normalized to the length of the cistron. (B) Frequency of the sites under positive selection.

Nucleotide diversity and selection by cistrons

Nucleotide diversity was measured per cistron, normalized to the length of the cistron for the 5 most variable poleroviruses and PLRV. The CPRT showed the highest nucleotide diversity followed by P0, P1, P3a, MP, P2, and CP (Figure 2.4A). Using SLAC and MEME, positive and negative selection sites were mapped across each cistron for the 5 most variable potyviruses and PLRV. In general, the abundance of negative selection sites across the genome was 15-fold higher than positive selection sites, showing that polerovirus genomes are primarily under negative selection. Sites under negative selection were measured across each cistron, normalized to the length of the cistron. Relative to the cistron, the CPRT had the most sites under negative selection followed by P0, P1, CP, P2, MP, and P3a (Figure 2.4B). The CPRT followed by P0 also had the most positive selection sites (dN/dS ratio > 1) (Figure 2.4C). Hypervariable cistrons contain the most negative and positive selections sites. In general, the CPRT is the most variable cistron while CP appears to be one of the most stable cistrons due to its low nucleotide diversity, high number of negative selection sites, and low number of positive selection sites. Overall, the CPRT and P0 appear to be hypervariable areas and thus likely viral determinants.

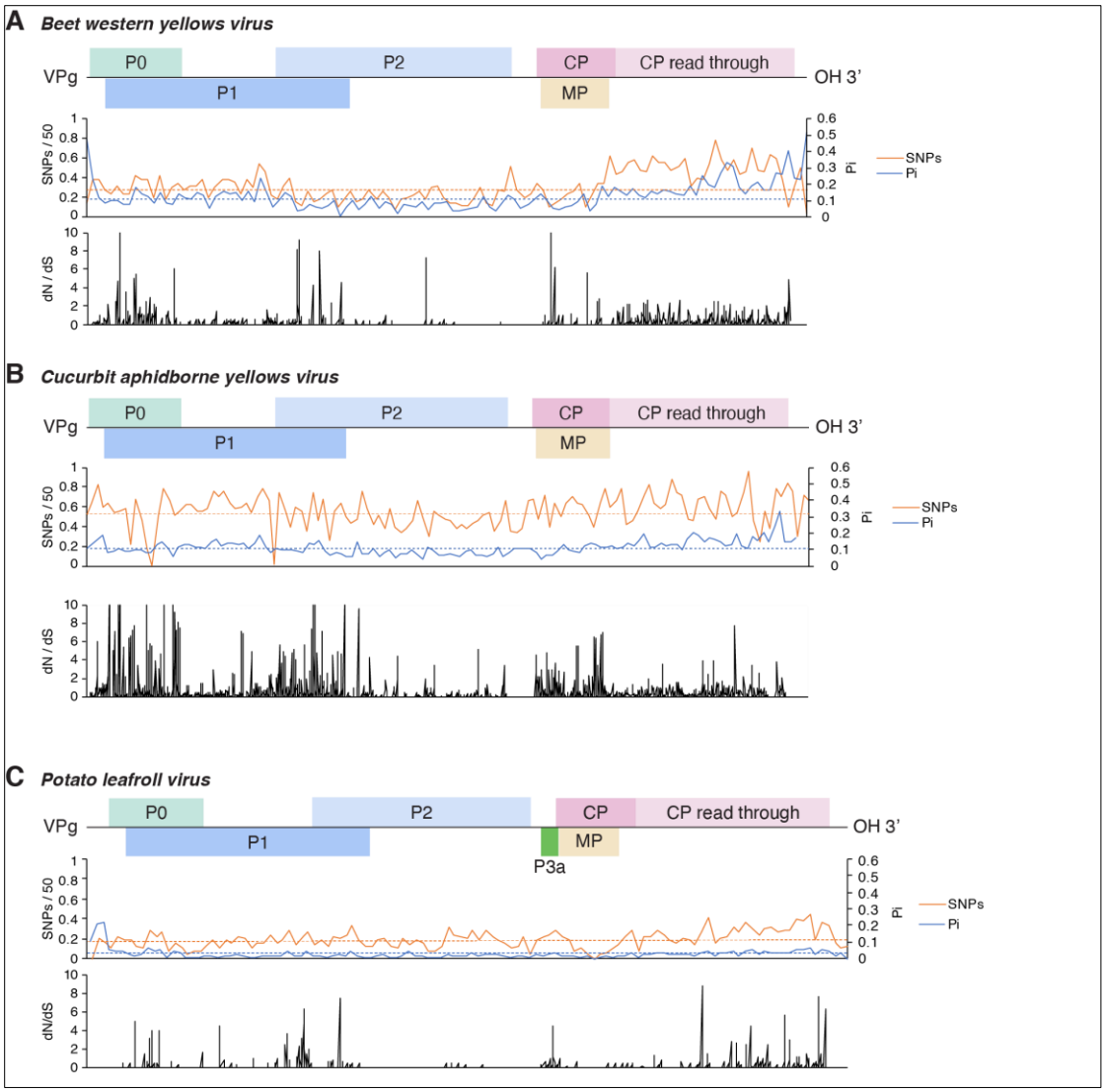

Figure 2.5. Genome-wide variation in Beet western yellows virus, Cucurbit aphidborne yellows virus, and Potato leafroll virus. Single nucleotide polymorphism (SNP) and nucleotide diversity (Pi), and the ratio of non-synonymous to synonymous changes (dN/dS) were estimated in 50-nt window. The average and a 99% confidence interval (p-value < 0.01) is indicated as a horizontal line. (A) Beet western yellows virus. (B) Cucurbit aphidborne yellows virus. (C) Potato leafroll virus.

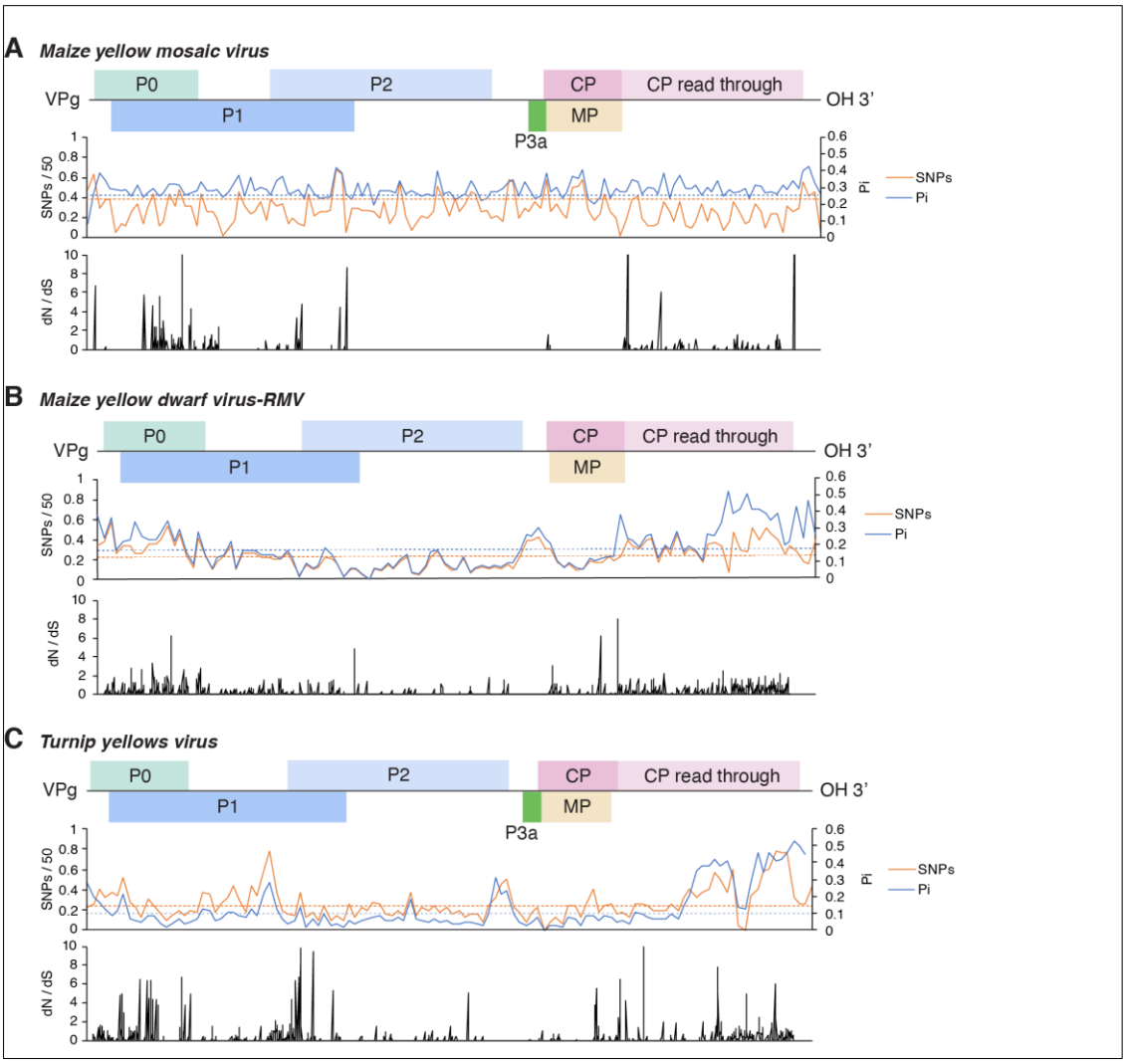

Figure 2.6. Genome-wide variation in Maize yellow mosaic virus, maize yellow dwarf virus-RMV, and Turnip yellows virus. Single nucleotide polymorphism (SNP) and nucleotide diversity (Pi), and the ratio of non-synonymous to synonymous changes (dN/dS) were estimated in 50-nt window. The average and a 99% confidence interval (p-value < 0.01) is indicated as a horizontal line. (A) Maize yellow mosaic virus. (B) Maize yellow dwarf virus-RMV. (C) Turnip yellows virus.

P0 and the CPRT are hypervariable

Variation in poleroviruses is often mapped only in new species or within all the isolates of a few select polerovirus species such as BYDV or SCMV. (Pagán and Holmes, 2010) This fact illustrates the need for studies investigating variation across all proteins in all poleroviruses. Here, SNPs and Pi were estimated in a 50-nt window to

determine whether nucleotide variation occurs randomly or in concentrated areas in the genome. A map of each polerovirus genome was created to visualize the variation distribution. SNPs and Pi were normalized and plotted against this genome to create an identity plot (Figure 2.5 and Figure 2.6). Variation is not distributed randomly across the genome and is instead concentrated in specific areas. The areas of high nucleotide variation and diversity in all 6 tested poleroviruses mapped to the terminal ends of poleroviruses containing protein 0 (P0) and the coat protein read-through domain (CPRT). Figure 2.5B, 2.5C, and 2.6A also showed peaks in the intergenic region (IR) and the protein 3a (P3a) region. All 6 poleroviruses showed a lack of variation in the P2 protein showing this area to be the most stable section of the genome.

In all viruses, areas of the genome under positive selection are ideal for evolution by increasing host range (Bedhomme et al., 2012). Using SLAC and MEME, each cistron was analyzed for the location of positive and negative selection sites. (Figure 2.5 and Figure 2.6). We found that areas of positive selection also mapped towards the terminal ends of the protein containing P0, protein 1 (P1), and CPRT (dN/dS ratio > 1, p-value ≤ 0.05). Figure 2.5B, 2.45C, 2.6A, and 2.6B exhibited areas of dense positive selection at the coat protein (CP) and movement protein (MP) overlap. Protein 2 (P2), P3a, and the IR had the least sites under positive selection compared to the whole genome. Negative selection sites followed the same pattern with the most occurring at P0, P1, and the CPRT and the least in P2, P3a, and the IR. This could explain why recombination between polerovirus species happens most frequently at the center of the genome near the IR.

Poleroviruses have two hypervariable areas located at the P0 and CPRT proteins evidenced by SNPs, Pi, and selection analyses, indicating these proteins may be important for host adaptation (Figure 2.4-2.6).

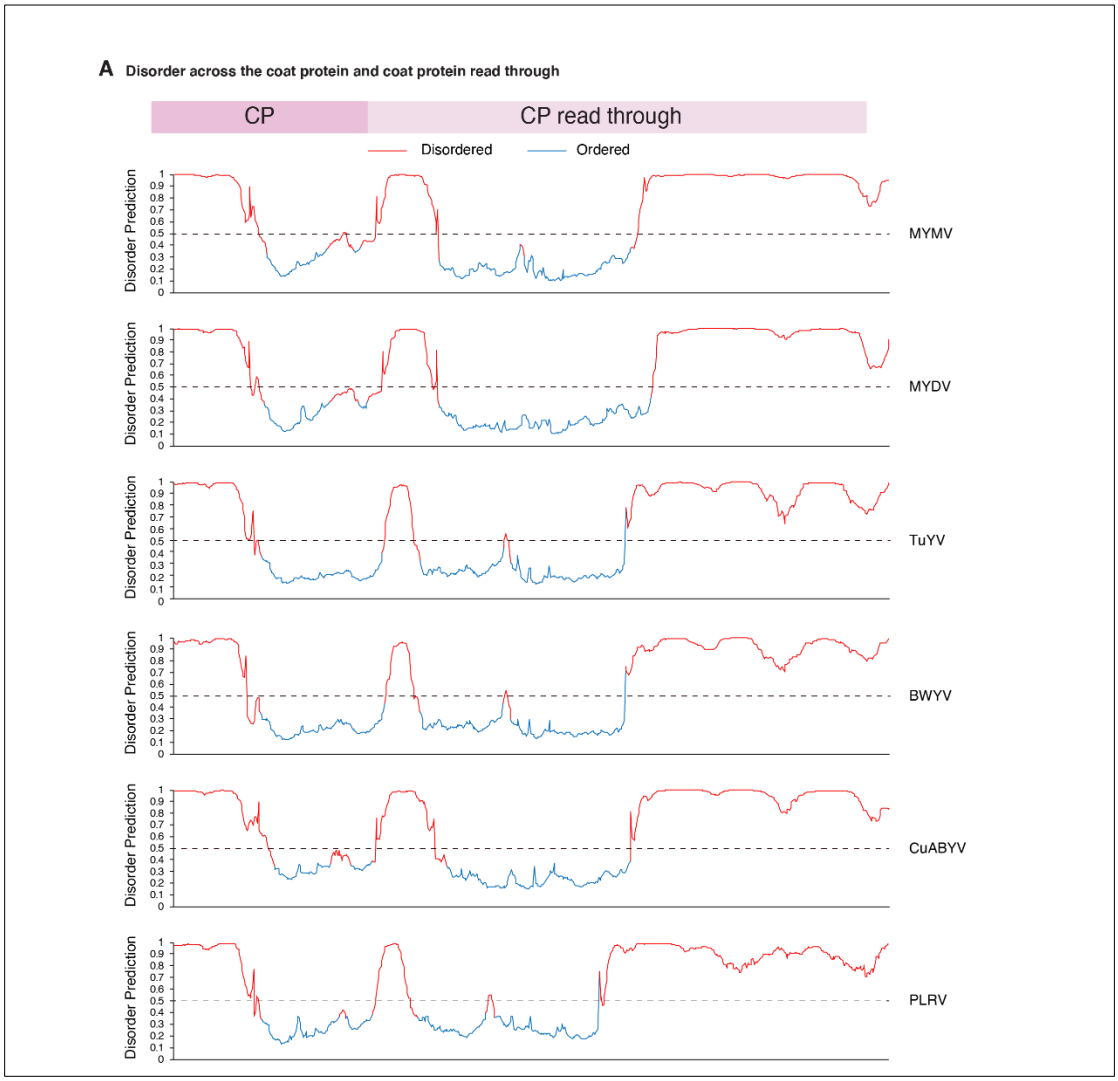

Figure 2.7. Disorder of CP-CPRT of top 5 most variable polerovirus and type species. Disorder across CP-CPRT mapped using MFDp with p=0.05 threshold representing disorder and order respectively. Colored based on MFDp disorder and order prediction.

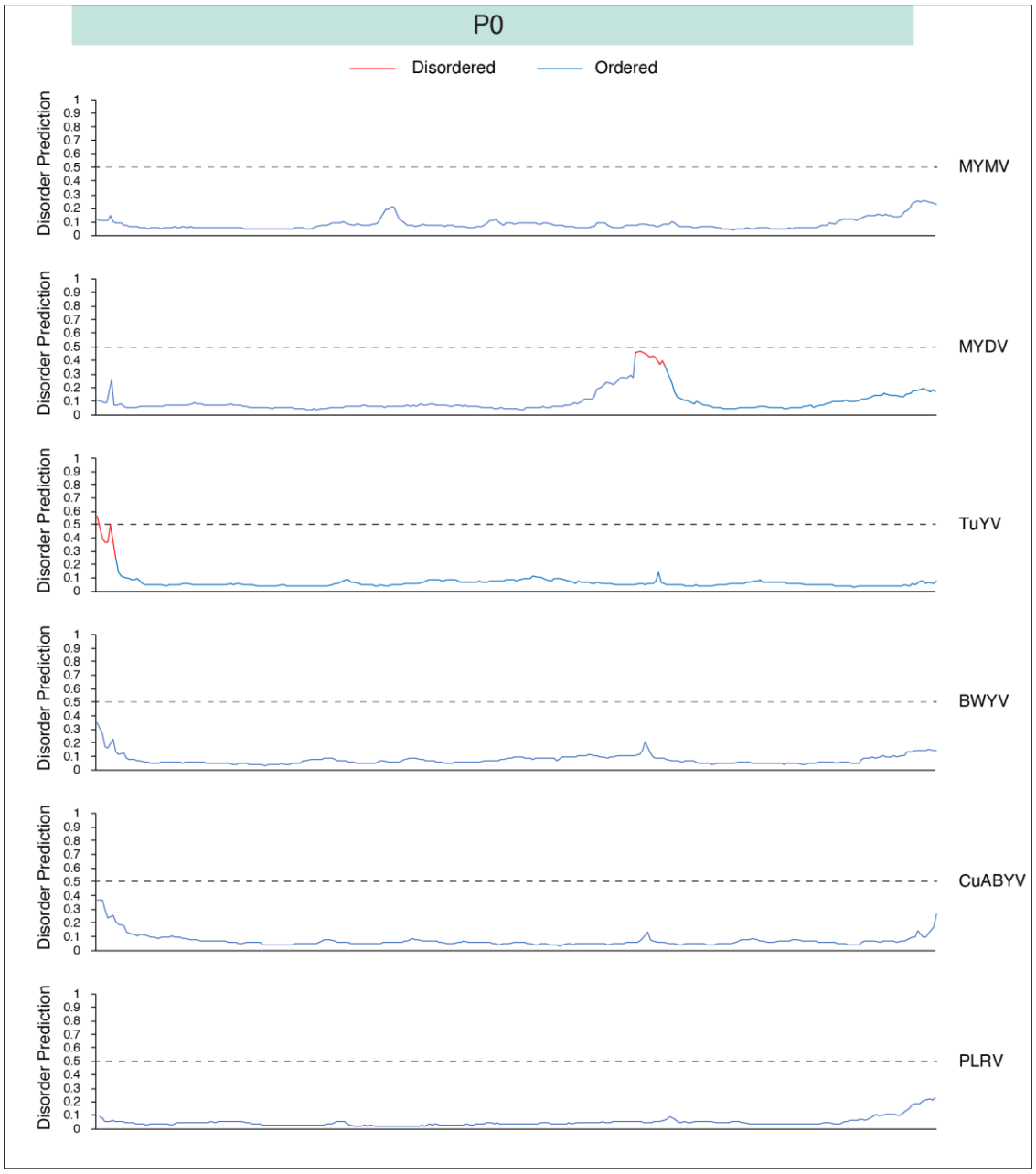

Figure 2.8. Disorder of P0 of top 5 most variable polerovirus and type species. Disorder across P0 mapped using MFDp with p=0.05 threshold representing disorder and order respectively. Colored based on MFDp disorder and order prediction.

The CP-CPRT is highly disordered while P0 is highly ordered

Intrinsically disordered proteins (IDP) and intrinsically disordered protein regions (IDPR) are often associated with protein-protein interactions as well as regulating important processes such as transcription, translation, and assembly of protein complexes (Szilágyi et al. 2008). For each of the 5 most variable poleroviruses and PLRV, the disorder of CP-CPRT for each reference sequence was measured using the Multilayered Fusion-based Disorder predictor (MFDp), a consensus-based disorder predictor. The N-terminus of the CP shows a long segment of disorder (>30 residues) ranging from 66-88 amino acids (Figure 2.7). The C-terminus of CP and the N-terminus of the CPRT also show an area of disorder ranging from 26-55 amino acids. The N-terminus of the CPRT has the longest stretch of disorder with a minimum of 213 amino acids and a maximum of 285 amino acids with a high degree of confidence. The CP-CPRT is on average 59% disordered. P0 disorder was calculated using MFDp similar to the CP-CPRT. All 6 poleroviruses showed that P0 is essentially entirely ordered, in contrast to the CP-CPRT (Figure 2.8). This suggests hypervariability does not correlate with a disordered structure. The areas of order and disorder are shared throughout the 6 poleroviruses indicating the genus likely shares a pattern of disorder and order across the CP-CPRT and P0 protein. This suggests the CP-CPRT may play a role in host adaptation by binding to several host and virus factors.

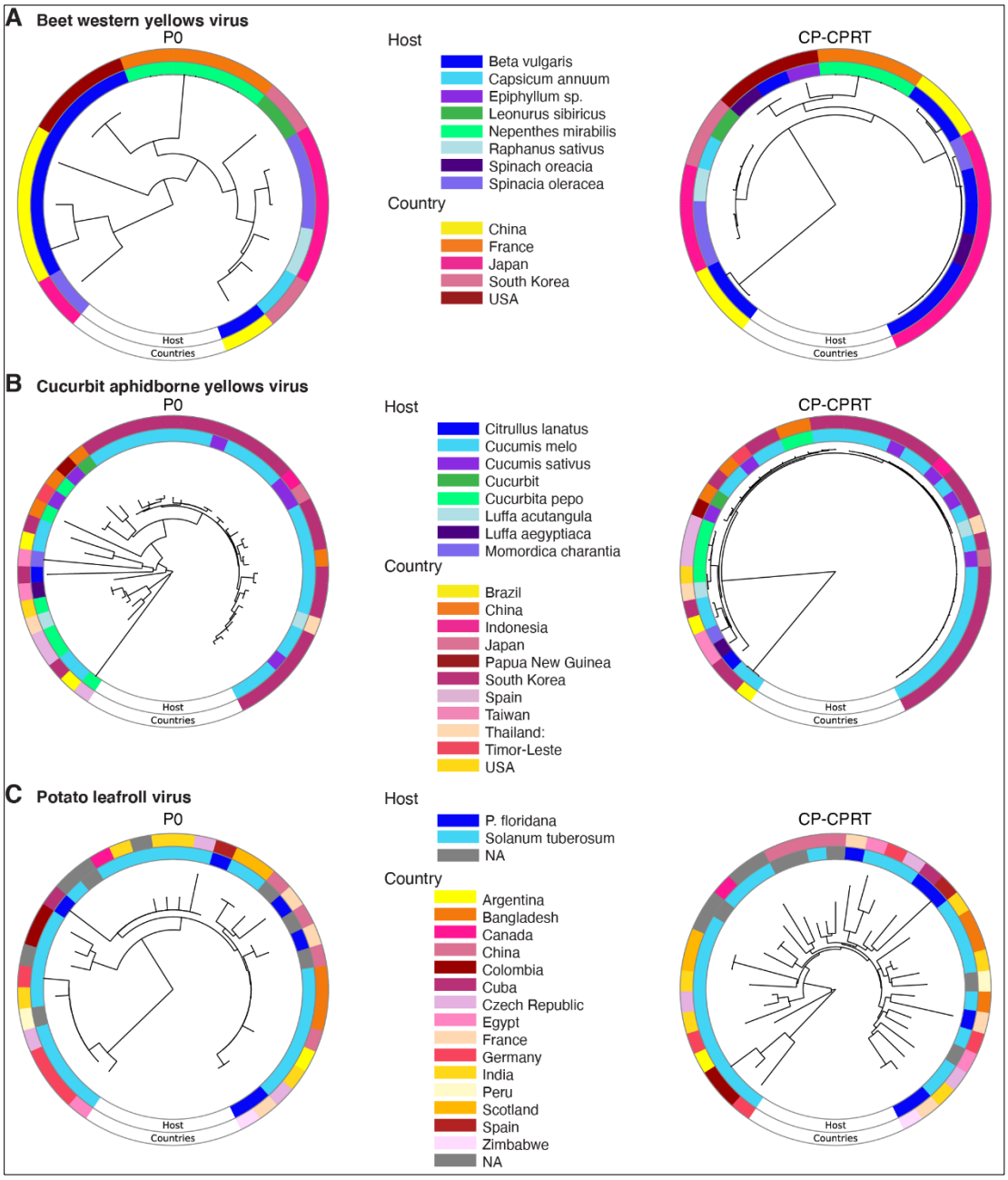

Figure 2.9. Phylogram based on P0 and CP-CPRT protein sequences. The neighbor-joining phylogenetic tree in the center was generated using MAFFT. Outer ring indicates country of origin and the inner ring the host. (A) Beet western yellows virus. (B) Cucurbit aphidborne yellows virus. (C) Potato leafroll virus.

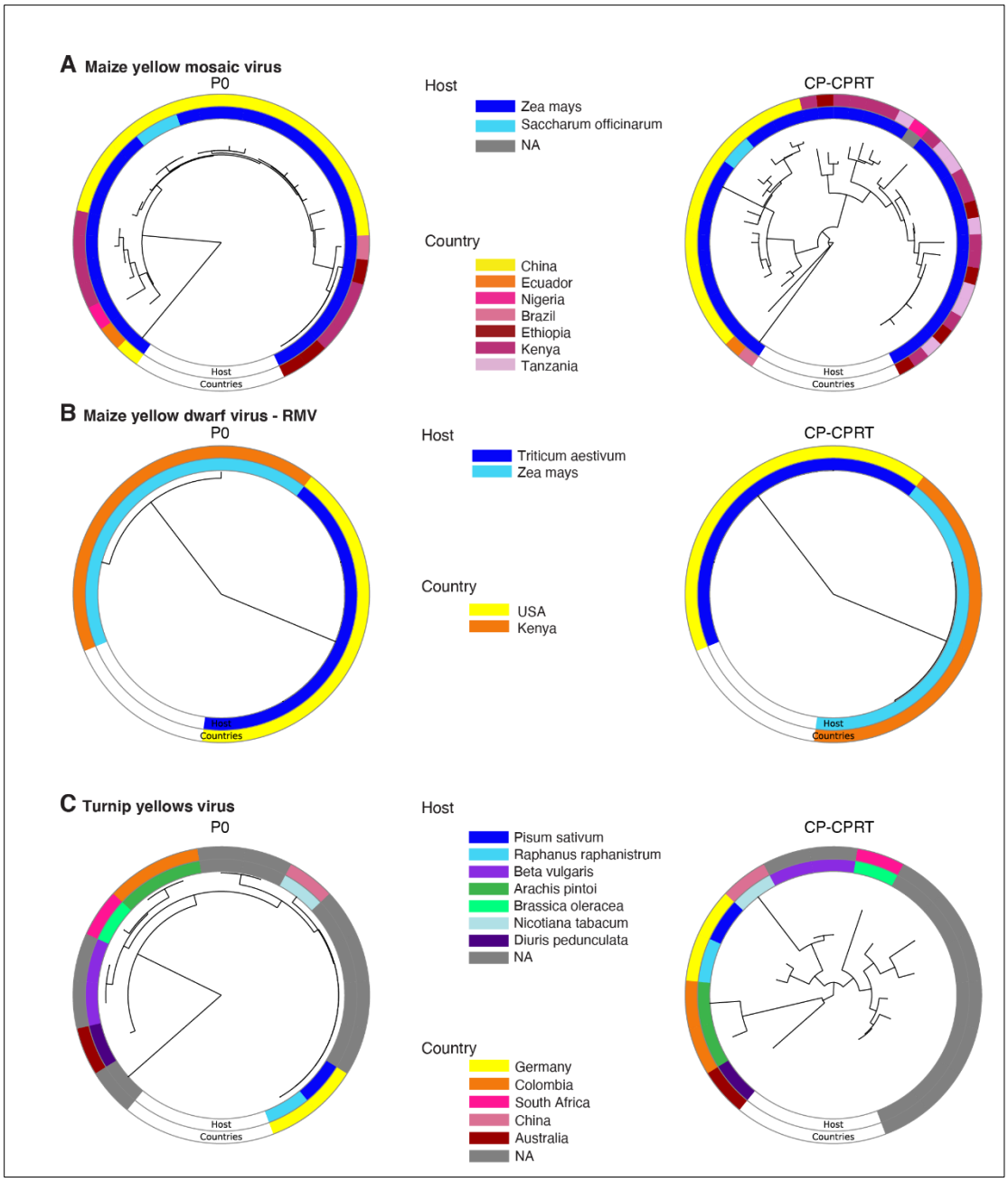

Figure 2.10. Phylogram based on P0 and CP-CPRT protein sequences. The neighbor-joining phylogenetic tree in the center was generated using MAFFT. Outer ring indicates country of origin and the inner ring the host. (A) Maize yellow mosaic virus. (B) Maize yellow dwarf virus-RMV. (C) Turnip yellows virus.

Polerovirus genetic diversity

Phylogenies for each of the 5 most variable viruses and PLRV were created to determine if hypervariable areas correlated with host and geographic origin of the virus. Separate phylogenetic trees were created based on either P0 or CP-CPRT protein sequences for each species (Figure 2.9 and Figure 2.10). Phylogenetic trees within each species showed vastly different structures depending on if they were based on P0 or CP-CPRT. The CP-CPRT phylogenies had greater numbers of clades and branches showing the protein is less conserved across isolates. This suggests the recombination frequently observed in poleroviruses directly affects the evolution and variation within each virus not only within species. Consistent with previous studies, accessions clustered together based on host rather than by country of origin. (Pagán & Holmes, 2010). However, for trees based on the CP-CPRT, accessions grouped less often by host and had a more random distribution. This suggests proteins involved in host adaptation and vector transmission requires more variation. MYDV-RMV had only two hosts so grouping by host was unclear. Grouping by host and P0 and CP-CPRT phylogenetic tree differences were consistent across the examined poleroviruses suggesting this is a pattern common to poleroviruses.

DISCUSSION

Poleroviruses face a wide array of host and vector factors that serve as evolutionary constraints. They must balance retaining both essential functions and genomic flexibility as they interact with a variety of host and viral proteins and RNA (Wan et al., 2015; Li et al., 2016). Variation occurs through several methods including nucleotide insertions, deletions, substitutions, and genomic recombination (Garcia

2018). Single nucleotide mutations are caused by viral RNA-dependent RNA polymerases during viral replication (Garcia-Arenal et al. 2001). However, mutations can have either positive or deleterious effects leading to them becoming fixed or removed from the viral population (Nigam et al., 2020). This variation enables poleroviruses to infect a broad range of hosts and can eventually lead to the creation of new species (Nigam et al., 2019). The speed of speciation is increased in poleroviruses because they are RNA viruses, which have faster mutation rates than DNA viruses. Further, poleroviruses often recombine across species and genera (Pagán and Holmes, 2010). These selection pressures result in mutations occurring non-randomly in specific, hypervariable areas of the genome.

The characterization of the whole polerovirus species has not been done before. In this study, we mapped variation of the top variable poleroviruses that have at least 3 full-genome accessions. The most hypervariable proteins found in both the SNP and Pi data were P0 and CP with CP mainly having its variation in the CPRT region. (Figure 2.5 & 2.6) This supports the idea that Polerovirus genomes are highly variable with this variation focused on the terminal ends of the monopartite genome (Boulila, 2011; Dombrovsky et al., 2013).

Screening for selection pressure and adaptive evolution is best accomplished comparing nonsynonymous to synonymous substitutions (dNdS). In the whole Luteoviridae, poleroviruses have been seen to possess the highest dNdS ratios which could reflect vector species that is responsible for virus transmission in polerovirus versus the other species in Luteoviridae.

Positive selection and recombination is known to make viruses evolve faster (Boulila, 2011). Within each protein coding region, P0 and CPRT had the most frequent sites under positive selection (Figure 2.4C). With that in mind, this explains why viruses in the Luteoviridae seem to evolve faster than other families of viruses and are one of the most successful plant viruses (Boulila, 2011). In contrast, CPRT had the highest negative selection between all of the other protein coding regions (Figure 2.4B). However, this goes against other data that say the CP, CPRT, and MP regions are normally highly conserved (Boulila, 2011; Pagán & Holmes, 2010). This can be explained by CPRT having frequent sites under both positive and a negative selection. Areas of the two coat protein structures created from CP and CP plus CPRT that create the structure of the virion most likely have highly conserved areas along with hypervariable. The hypervariable areas allow for host adaptation and viral evolution.

P0 and P1 follow a similar pattern all throughout Figure 2.4. This can be explained by P0 having a majority of its nucleotides overlapped with P1. Figure 2.5 & 2.6 along with Pagán and Holmes found that there usually was no difference between overlapped and non-overlapped protein regions (2010). However, both we also found the CPRT, which is non-overlapped, to have higher rates of substitutions. This might be related to functionality of the protein. P0 functions as an RNA silencing suppressor and where P1 contains important sites for the virus: the VPg domain, the location of frameshift to create RDRP, and the site for proteinase activity. Also, the 5’ end of CP overlaps with MP making it important to the virus as well. These regions can easily be compromised by mutations. But the non-overlapped region of the coat protein contains

the CPRT which is a lot more variable, has a higher rate of mutations, and was under high negative selection (Figure 2.4).

Interestingly, P3a had the highest nucleotide diversity in Figure 2.4A. This can possibly explain by the support that intergenic regions (Nigam & Garcia-Ruiz, 2020) higher rates of nucleotides substitutions on average.

Intrinsically disordered proteins (IDPs) and intrinsically disordered protein regions (IDPRs) are important for several essential biological functions, including protein-protein interactions, transcription, and signal transduction (Lieutaud et al., 2016). These IDPs and IDPRs lack a fixed 3D shape giving them greater flexibility and plasticity than many proteins. The CP-CPRT is a highly disordered (Figure 2.7) protein in comparison to P0 (Figure 2.8). The disordered regions correlate with aphid transmission, systemic movement, and long-distance movement of viral particles (Gray et al. 2008). The disorder of this protein and these specific areas would explain previous findings where mutations in these areas were varied and often host dependent (Gray et al. 2008). This suggests a correlation between disorder and host adaptation. Poleroviruses must be able to interact with both vector and host proteins in order to ensure infection. Disorder in areas that interact with host and vector proteins could enable infection of new hosts and to avoid deleterious effects from introduced mutations. P0 is hypervariable but with a rigid tertiary structure. This supports the idea that its role of a silencing suppressor requires specific binding with the host S phase kinase-associated protein 1 (SKP1) proteins that lead to the downstream degradation of AGO1 (Li et al., 2019). The disordered structure in the CP-CPRT indicates that these proteins are designed to bind

to a vast number of genetic partners and require the genomic flexibility to ensure pathogenicity.

Viruses and their hosts are trapped in an evolutionary arms race as they both seek to out evolve the other. This co-evolution leads to changes at the genus level as recombination and adaptation lead to the formation of new species (Pagán and Holmes, 2010). However, these evolutionary pressures can also be seen at the genomic level (Nigam et al., 2019). The selection pressures exerted on viruses by vectors and hosts factors leads to the accumulation of mutations in specific proteins. These proteins are viral determinants of host evolution (Nigam et al., 2019). Recombination is the main mechanism used to create diversity amongst poleroviruses because it creates bigger effects than mutations. This can threat the viral controls that exist today. (Boulila, 2011; Pagán & Holmes, 2010) Understanding recombination and how it contributed to the evolution of poleroviruses will be beneficial. Recombination can happen between multiple viruses or even between the virus and host. Factors that affect recombination are how the molecule is structured and the ability of replicase to switch templates. Between 66% and 100% of recombination have been seen to occur at the intergenic region between the RDRP and the CP (Pagán & Holmes, 2010). Because of this, we decided to create phylogenies from the sequences of the terminal end proteins: P0 and CP with CPRT (Figure 2.9 & 2.10). We found that the trees created from the same virus, but out of proteins at each terminal end created vastly different trees. We determined that recombination did play a part in evolution of polerovirus species consistent with previous studies (Boulila, 2011; Pagán & Holmes, 2010). These phylogenies show that

the RNA of the viruses are taxonomically different but the viruses still depend on each other in the context of the whole polerovirus species.

By approaching variation at the genus level, we were able to determine the overall variation pattern within all polerovirus species rather than only within a specific species. The polerovirus genome is highly variable with the CPRT and P0 showing the highest variation and positive selection sites (Figure 2.4). Phylogenies based on these proteins show vastly different viral evolution, consistent with a high number of recombination events leading to vastly different genomic sequences. This genomic variation correlates with the host of the virus, so viruses are most closely related to those with similar host families rather than geographic origin (Figure 2.1, 2.9, & 2.10). Characterizing variation and thus viral determinants has immense impact on diagnostics and resistance breeding. Understanding which genes are conserved or variable can lengthen the time before resistance is broken and help design universal polerovirus diagnostic tests.

MATERIALS AND METHODS

All computational analysis was conducted using the high-performance computing nodes at the University of Nebraska-Lincoln Holland Computing Center (https://hcc.unl.edu/).

Nucleotide Sequences

Genomic sequences for all polerovirus species were downloaded from NCBI on November 14th using customized scripts based on Entrez Programming Utilities (E-utilities; https://www.ncbi.nlm.nih.gov/books/NBK25500/). One accession for each species was chosen as the reference genome. This accession was either the NCBI-

designated reference accession for the species, or, if NCBI did not have a designated reference genome, then the accession with the longest sequence was chosen (Supplementary Table 1). The reference genome was used to determine the coordinates for each cistron. From the downloaded accessions, all accessions with less than 95% of the reference genome were removed. Next, only species with at least three accessions were used to ensure meaningful statistical comparisons (Shen et al., 2010). The remaining 25 polerovirus species were used for all downstream analyses.

Phylogenetic Tree

Consensus sequences were derived for each species using custom scripts. Consensus sequences were combined and aligned using the online form of MAFFT version 7 (Multiple Alignment using Fast Fourier Transform) to form a Neighbor Joining tree (https://mafft.cbrc.jp/alignment/server/). Newick files of this alignments were transferred to Figtree version 1.4.3. for visualization (http://tree.bio.ed.ac.uk/software/figtree/) (Rambaut, 2009).

Genomic Diversity

For all poleroviruses, alignment files (.aln) from MAFFT were downloaded and analyzed for single nucleotide polymorphisms (SNPs) as described (Nigam et al., 2019) and nucleotide diversity (Pi) in a 50-nt window. Nucleotide diversity was analyzed using Tassel version 5.0 (Bradbury et al. 2007). For both SNPs and Pi, a 99% confidence interval was estimated (Hazra, 2017). SNPs and Pi were mapped across the genome for the five most variable poleroviruses and PLRV along with a 99% confidence interval for both SNPs and Pi.

Selection Analysis

Positive and negative selection sites were identified for each cistron for the 5 most variable poleroviruses and PLRV. For each cistron, sequences were obtained using custom python scripts. To obtain P1-P2 coding sequence, the frameshift nucleotide was repeated to allow for P1-P2 translation. For the CP-CPRT, the CP stop codon was changed from UAG to CAG to allow for translation. Sequences were translated using EMBOSS Transeq online (https://www.ebi.ac.uk/Tools/st/emboss_transeq/). Sequences were aligned using MAFFT and alignment files inputted into Single-likelihood ancestor counting (SLAC) and MEME tools at http://www.datamonkey.org/. A significance level ≤0.05 and >0.95 posterior probability was used for both online versions of SLAC and MEME (Murrell et al., 2012). Abundance of positive and negative selection sites were normalized to the length of the cistron. For the P1-P2 fusion protein and the CP-CPRT, sites were counted only for the sections of protein that did not overlap with P1 and the CP, respectively. P3a was normalized to the length of the window to avoid variation overestimation.

P0 and CP-CPRT Geographic Origin and Host Range

For selected viruses, a phylogram was generated based on either available P0 or CP-CPRT polyprotein sequences as described (Nigam et al., 2019).

Protein Disorder

Disorder and order were mapped for P0 and the CP-CPRT polyproteins using the Multilayered Fusion-based Disorder predictor (MFDp). MFDp (http://biomine.cs.vcu.edu/servers/MFDp/) is a meta-predictor composed of several different disorder predictors, primarily DISOPRED, DISOclust, IUPRED–S, and

IUPRED-L (Mizianty et al., 2010). The reference accession for the selected viruses was used as inputs. Regions were colored based on predicted order and disorder and plotted by their disorder probability. The threshold of 0.5 represents a false positive rate of 5%. For PLRV, P1 and VPg disorder and order were mapped similarly using the accession P11622.

CHAPTER 3

SILENCING SUPPRESSION ACTIVITY OF A POLEROVIRUS P0 PROTEIN

Holste, N. and Garcia-Ruiz, H.

INTRODUCTION

Maize (Zea mays L.) is an important crop used for food, animal feed, and biofuel production. As a result, maize is the number one crop in the world (Shiferaw et al., 2011). However, there are barriers to producing enough maize to feed a growing population. For example, maize is susceptible to over 50 known virus species that cause a reduction in quality such as ear development and size (Lapierre et al., 2004) and cause a yield loss of up to 60%. Among these is a detrimental disease called maize lethal necrosis disease. The disease is characterized by the combination of several maize viruses infecting one plant and leads to yield losses ranging from 30% to 100% each crop cycle (Sibanda, 2015). Originating in Kansas and Nebraska in the 1970's (Niblett & Claflin, 1978), maize lethal necrosis has since been eradicated in the United States. However, in 2011 maize lethal necrosis was detected in sub-Saharan Africa, (Adams et al., 2013; Mahuku et al., 2015; Wangai et al., 2012). This is concerning because about 80% of all sub-Saharan farmland is dedicated to growing maize (Dawson et al., 2016; Frankema, 2014). All efforts towards breeding resistance have not helped as the virus easily mutates once a resistant variety is found. The yield loss from maize lethal necrosis threatens the economy and ability to nourish the people of sub-Saharan African countries like Kenya and Rwanda. (Wamaitha et al., 2018)

Generally, maize lethal necrosis is caused by the coinfection of at least two viruses. The consistent virus is always maize chlorotic mottle virus (MCVM), a Machlomovirus. The other virus is typically any member of the genus Potyvirus such as sugarcane mosaic virus (SCMV), Johnson grass mosaic virus (JGMV), or wheat streak mosaic virus (WSMV) (Wamaitha et al., 2018). When these maize viruses co-infect the same plant, they cause severe maize lethal necrosis disease (Niblett & Claflin, 1978;

Uyemoto, 1980; Wangai et al., 2012). However, Wamitha et al. (2018), concluded that an alternative combination could also cause maize lethal necrosis. Using samples collected in Kenya, they detected MCMV in combination with poleroviruses (Wamaitha et al., 2018). In most of the samples, up to 4 viruses were detected from individual plant samples, and a particular strain of polerovirus was detected in all samples (Wamaitha et al., 2018). This polerovirus most similarly resembles maize yellow mosaic virus (MaYMV) because it shares 97% sequence similarity (Wamaitha et al., 2018).

RNA silencing is used in plants, animals, and fungi as a regulator of gene expression. In plants, this same system is used as a defense system against foreign nucleotides—viruses (Alvarado & Scholthof, 2009; Cao et al., 2014; Garcia-Ruiz et al., 2015; Szittya & Burgyán, 2013). RNA silencing induces the formation of 21 and 24 nucleotides by Dicer-like proteins from strands of the virus genome (Ding & Voinnet, 2007). These 21 and 24 nt small RNAs (siRNA) are loaded on to Argonaute (AGO) proteins. This siRNA and AGO combination is called RISC. RISC can target sequences matching the siRNA loaded onto it. Once matched, sequence degradation is initiated, inactivating any new virus particles (Garcia-Ruiz et al., 2010, 2015).

Wamitha et al. (2018) predicted that poleroviruses could be contributing to the detrimental nature of maize lethal necrosis. It has been suggested that polerovirus co-infection with a non-phloem limited virus increases symptom severity due to the nature of their RNA silencing suppressor protein. (Baumberger et. al., 2007) It is known that P0 protein is the silencing suppressor of the genus Polerovirus (Krueger et al., 2013). However, not all polerovirus P0 proteins have been characterized and the mechanism of action of P0 to suppress the host viral defense is still a matter of research. Silencing

suppressors like P0 counteract RNA silencing by leading to the degradation of AGO1 (Baumberger et al., 2007), but it is suggested they could target more AGO proteins. Silencing suppressors from other geneses of viruses target other areas of the RNA silencing system. In maize lethal necrosis, the silencing suppressor for MCMV is not known. The potyviral silencing suppressor, HC-Pro, is known and highly studied. They are known to bind to siRNA making them unavailable for AGO proteins to attach and degrade matching sequences. (Fukuzawa et al., 2010; Kasschau & Carrington, 2001) If MCMV, potyviruses, and poleroviruses target different areas of the RNA silencing system, this would suggest this is the cause of a more detrimental disease.

Since viral pathogenicity is related to RNA silencing suppression (Vance & Vaucheret, 2001), characterizing P0 will lead us to understanding the pathway poleroviruses of maize lethal necrosis can target. Therefore, this work aims to characterize P0 from the MaYMV strain obtained from Kenyan samples isolated by Wamaitha et al. (2018). Understanding the vital proteins involved can provide insight into genome-wide polerovirus function and narrow down the role of poleroviruses in maize lethal necrosis. It could also enable us to target management strategies for maize lethal necrosis in sub-Saharan Africa.

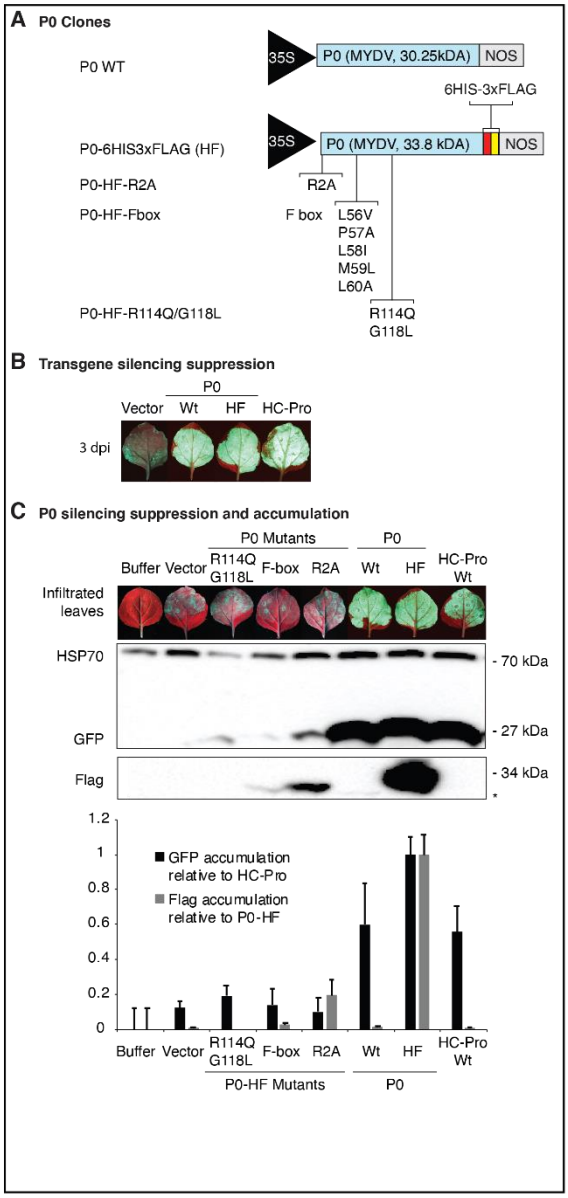

Figure 3.1. GFP transgene silencing suppression and P0 protein accumulation (A) Illustration of MaYMV P0 clones found between the 35S promoter and the nopaline synthase (NOS) terminator on the pMDC32 vector. A 6xHis-3xFLAG (HF) tag was added to the C-terminal side of the protein. P0 inactivating mutations (R2A, F-box, and R114Q/G118L) are indicated. F-box is a replacement of all amino acids that create the F-box-like motif of poleroviruses. (B) Suppression of RNA silencing by wild type (WT) and HF-tagged P0 at 4 days post co-infiltration with ssGFP in *N. benthamiana* leaves. An empty vector was included as negative control and HC-Pro, a potyviral silencing suppressor, as positive control (C) Protein expression and suppression of RNA silencing by wild type (WT), HF-tagged P0, and tagged mutants 3 days post-infiltration with ssGFP in *N. benthamiana* leaves. Buffer solution and empty vector are included as negative controls, and HC-Pro as a positive control. Western blot for GFP and

Flag expression (from what) after 3 days post-infiltration. Expected size for GFP is 27 kDa, and P0 (as detected by anti-Flag) is 32 kDa. Heat Shock Protein 70 (HSP70, 70 kDa) was used as a loading control. The asterisk indicates P0 degradation products at about 25 kDa. (D) GFP and FLAG signal was normalized to HSP70 signal and plotted. Representative data from one of 12 replicates is shown.

RESULTS

P0 Tagging and Mutational Inactivation

To test the role of MaYMV P0 (hereafter called P0) in pathogenicity, we created control and mutant constructs each containing a 6xHis-3xFLAG tag (HF) at the C terminus of the P0 sequence and expressed under the 35S promoter contained on the pMDC32 vector (Figure 3.1A). Before we created the mutants, we tested whether silencing suppression remained intact after adding the HF tag using a single-stranded green fluorescent protein (GFP) transgene in wild-type (WT) *N. benthamiana* following a standard assay that measures GFP fluorescence as the output of successful silencing suppression (Johansen & Carrington, 2001). At 3 days post infiltration, GFP fluorescence from P0-HF control was comparable to WT P0. As expected, the P0-HF control and WT P0 were both as bright as the positive control HC-Pro, while the negative control showed no fluorescent signal (Figure 3.1B). These results indicate that the HF tag did not affect transgene silencing suppression activity of P0.

To test the effect of each of these domains on P0-HF activity, we created three mutant constructs (hereafter called suppressor-deficient mutants). In P0, genetic analysis showed that amino acid 2 is a highly disordered protein and a necessary protein binding region. The F-box like domain consists of amino acids 56 to 60 and is necessary for transgene silencing suppression (Pazhouhandeh et al., 2006). Genetic analysis also showed regions of high positive selection at amino acids 114 and 118.

Positive selection shows that amino acids can change without the virus automatically correcting the mutation (Nigam et al., 2019). For the first construct we mutated R2A. For the F-box like domain, we mutated the amino acid sequence LPLML to VAILA. For the third construct, we mutated R114Q, and G114L. Results from standard transient assays of GFP co-infiltrated with P0, mutants, or controls indicated that all mutants were no longer capable of transgene silencing suppression activity (Figure 3.1C). As expected, GFP accumulated lower in the suppressor-deficient mutants compared to P0-HF and similar to the vector only control, indicating that all mutants could no longer suppress silencing. Using an anti-Flag antibody, P0-HF was detected in infiltrated leaves. Bar graphs with standard deviation error bars were created to quantify the GFP and FLAG antibody results. The GFP results match the GFP visualized. The FLAG results indicated the P0 protein is present and stable. Suppressor deficient mutants were not found at detectable levels except R2A. R2A is a stable, yet inactive mutant.

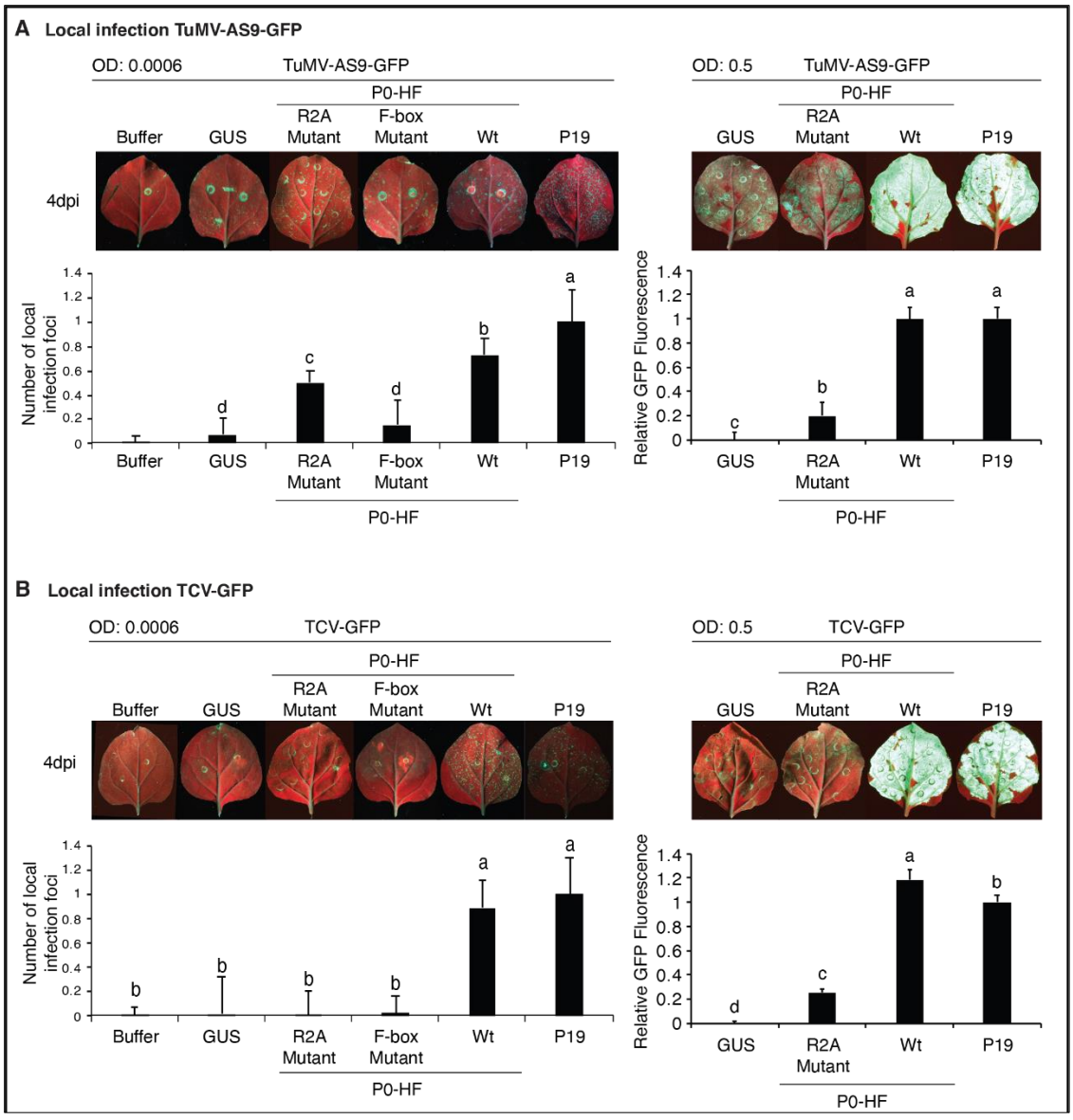

Figure 3.2 Virus infection site distribution in inoculated leaves of *N. benthamiana*. Plants were inoculated by agrobacterium with negative controls, buffer and GUS, treatments, P0-HF and P0-HF F-box mutant, and positive control, P19 (OD= 0.5). These were co-infiltrated with either (A) TuMV-AS9-GFP, suppressor-deficient TuMV, or (B) TCV-GFP (OD=0.0006). The images represent the leaves with each co-infiltration at 4dpi under UV light. Each GFP fluorescent spot represents the initial site of infection. The bar represents the average and standard error of three repetitions with 18 plants each repetition counting spots at 4dpi in a 2cm by 2cm section.

P0 restores pathogenicity to two viruses lacking their natural silencing suppressors

To test if P0 could act as a silencing suppressor in other viruses, P0-HF was co-infiltrated with Turnip mosaic virus and Turnip crinkle virus, both lacking their natural silencing suppressor (Figure 3.2). Again, the standard transgene silencing suppression assay was used. P0-HF accumulated to similar levels as the positive control P19 in both assays, indicating that P0-HF restored pathogenicity just as well as the natural silencing suppressor could. In contrast, the suppressor-deficient mutant had a reduction in foci, like the negative control. The results indicate that P0 can restore virulence to suppressor deficient viruses of different geneses, further indicating that P0 is a silencing suppressor.

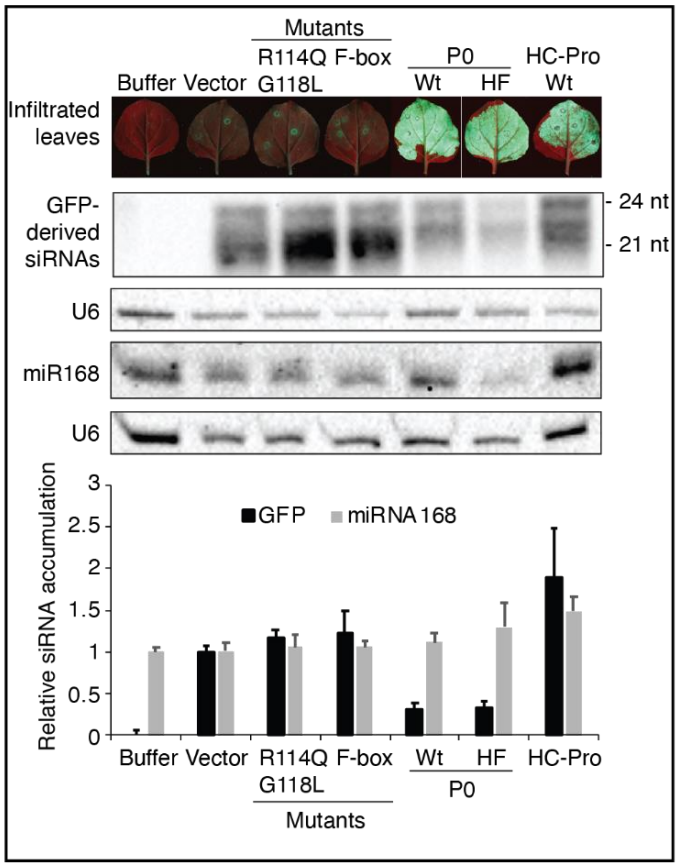

Figure 3.3 Effect of P0 protein on GFP-derived siRNA in wild type *N. benthamiana* leaves. P0 was co-infiltrated (OD=0.5) with GFP (OD=0.5). The images represent the leaves with each co-infiltration at 4dpi under UV light. siRNA was extracted at 4dpi. Buffer and vector were negative controls as described earlier. HC-Pro Wt was the positive control as described earlier. RNA was extracted and analyzed by northern blot analysis. GFP-derived siRNA and miR168 was probed for detection. The housekeeping gene, U6, was probed for as a loading control that all data is normalized to in the bar graph.

P0 reduces cellular and virus-derived siRNA

To understand the mechanistic activity of P0, P0 was co-infiltrated with GFP and extracted RNA at 3 days post infiltration (dpi) (Figure 3.3). We performed a northern blot analysis on small RNA and probed from GFP, a housekeeping gene, U6, and a primary siRNA, miR168. miRNA 168 is known to be a primary small RNA. GFP-derived small RNA represents secondary virus derived siRNA. There was a reduction in GFP-derived

siRNA. P0 caused a reduction in the accumulation of virus-derived small interfering RNAs and some cellular siRNAs. There was no effect found on this primary small RNA, indicating that the siRNA effect is only from secondary virus-derived siRNA.

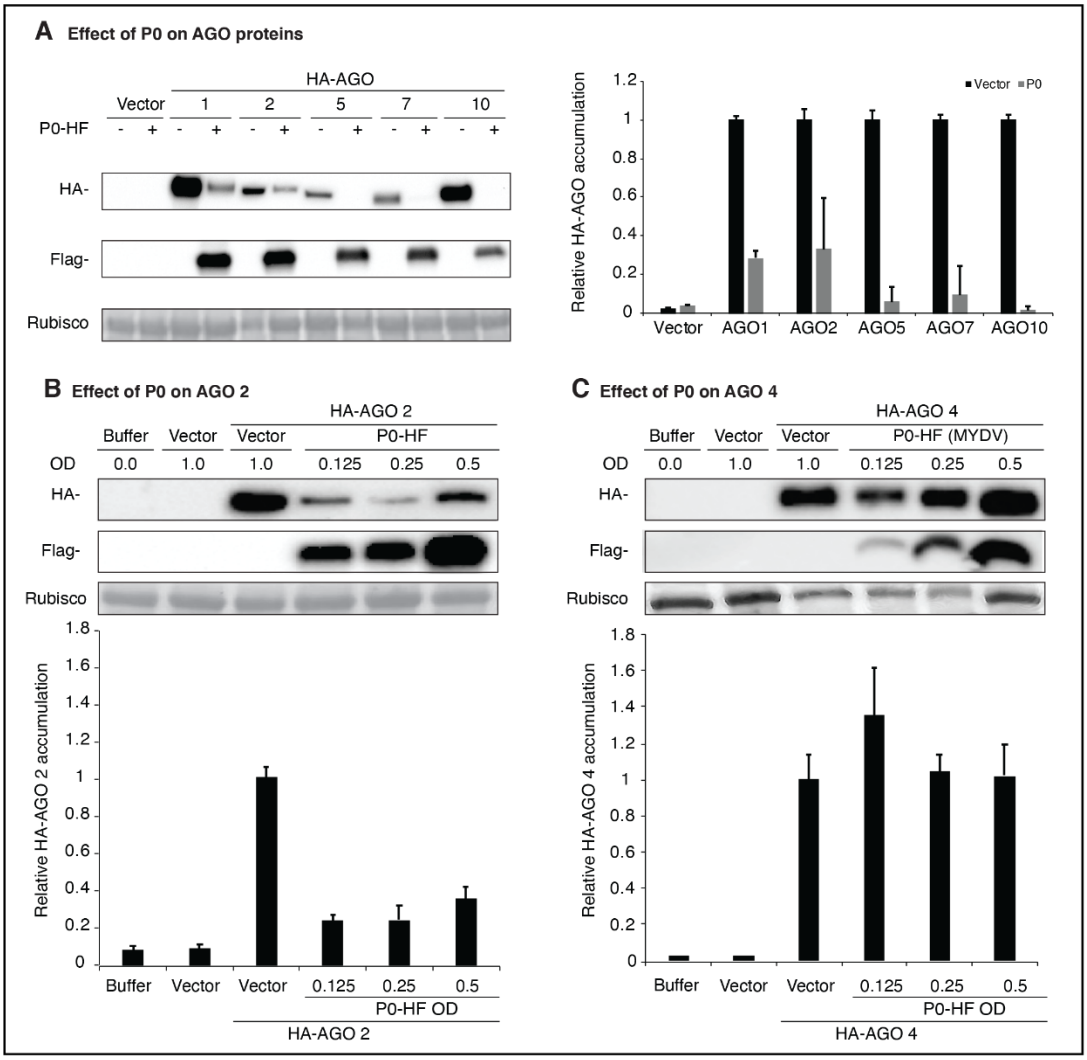

Figure 3.4 Effect of P0 protein on various Argonauts (AGOs) in wild type *N. benthamiana* leaves. (A) HF-tagged P0 was co-infiltrated with HA-tagged AGOs 1, 2, 4, 5, 7, and 10. Protein was extracted collected at 2 days post infiltration. The buffer solution (vector -), an empty vector (vector +), and an empty vector co-infiltrated with various AGOs (AGO # -) were used as negative controls. Anti-HA probed for AGO expression while Anti-Flag probed for HF expression.

Rubisco stain was used as a loading control. The addition of P0 resulted in a decrease in AGOs 1, 2, 5, 7, and 10. AGO 4 had no effect with the addition of P0. The graph shows these results compared to vector + AGO for each AGO. (B) Due to inconsistent results of AGO2 with P0, a dose response curve was performed. Leaves were co-infiltrated with varying concentrations of P0 and AGO2. The same negative controls, probes, and stain as (A) were used. Overall, it was concluded that P0 does produce a decrease in AGO2.

P0 reduces accumulation of several Argonaute proteins.

Of the 28 polerovirus species, 11 have confirmed that P0 is the silencing suppressor. For only 5 of the 11 species, P0 is known to target AGO1, a component of the RNA-induced silencing complex (RISC), for degradation. These species include Beet western yellows virus (Baumberger et al., 2007), Brassica yellows virus (Y. Li et al., 2019), Cucurbit aphid-borne yellows virus (Bortolamiol et al., 2007), Cotton leafroll dwarf virus (Agrofoglio et al., 2019), Cereal yellow dwarf virus (both -RPS and -RPV) (Almasi et al., 2015), and Potato leafroll virus (Zhuo et al., 2014). The mechanism of P0 in all other polerovirus species is unknown. However, it has been suggested that P0 could also target other AGO proteins in the complex that are responsible for siRNA activity and RNA silencing. To understand the effect of P0-HF on AGO proteins, we co-infiltrated them with HA tagged AGO 1, 2, 4, 5, 7, and 10 (Figure 3.4A). Anti-Flag and Anti-HA were used to visualized HF and HA, respectively. As expected, accumulation of AGO 1 dropped when P0-HF was added. AGO 5, 7, and 10 also decreased to almost no visible accumulation. AGO 2 dropped in accumulation, but not reliably. To understand the effect of P0-HF with AGO2, a dose response curve was generated (Figure 3.4B). P0 was added to AGO2 at differing concentrations. Although the effect in accumulation was not linear, P0-HF still reduced accumulation of AGO2 at all concentrations. Due to high accumulation of AGO4, a dose response curve was

performed with varying concentrations of P0-HF infiltrated with AGO4 at constant concentrations (Figure 3.4C). However, P0-HF has no effect on AGO4.

DISCUSSION

The MaYMV KARLO contains a strong silencing suppressor at protein P0 (Figure 3.1B). Three mutants were developed to elucidate the mechanistic activity of P0 (Figure 1A). We confirmed that P0 is a silencing suppressor of the MaYMV isolate (Figure 3.1B). All P0 mutants showed reduced activity and stability except for the R2A mutant (Figure 3.1C). This stable, inactive mutant could therefore be used to explain the effects of suppressed P0 activity compared to no activity or absence of the protein.

The mechanistic activity of the polerovirus P0 isolate compared to the inactive mutants or negative controls was found to decrease siRNA accumulation on both cellular and virus-derived RNA. (Figure 3.3). However, the details of the general siRNA biogenesis pathway are not well known at this time. What is known is that 21 and 24 nucleotide (nt) siRNA are formed by Dicer-like proteins that cut the double stranded RNA (Bologna & Voinnet, 2014; Gasciolli et al., 2005). Plants infected with virus accumulate 21 nt, 22 nt, and 24 nt siRNAs from the virus. (Donaire et al., 2009; Garcia-Ruiz et al., 2010, 2015a; Harvey et al., 2011; Qi et al., 2009; Wang et al., 2011) This polerovirus P0 protein lead to the degradation of both siRNA sizes. We concluded that P0 is degrading secondary siRNAs.

P0 effectively leads to the degradation of important developmental and anti-viral proteins. When we co-infiltrated AGO 1, 2, 5, 7, and 10 in separate assays with P0, we found the accumulation was decreased when in the presence of P0 from the MaYMV isolate (Figure 3.4). AGO proteins are a component of the RNA-induced silencing complex that cleaves RNA that matches the siRNA strand attached (Carbonell et al.,

2012; Schuck et al., 2013). If siRNA is not bound to an AGO protein, the cell naturally degrades the siRNA, making unbound-siRNA unstable. (Ding & Voinnet, 2007) These findings show that P0 affects the stability of siRNA.Therefore, if AGO proteins are reduced in accumulation in the presence of P0, it would affect the stability of virus-derived siRNA in the cell. We show that P0 has no effect on miRNA168 which is primary siRNA. Because there was no effect on miRNA168, P0 has no effect on primary siRNA.

The diversity amongst polerovirus P0 protein makes it difficult to understand its mechanistic activity. Several poleroviruses that contain P0 and have silencing suppression activity have been described. (Almasi et al., 2015; Csorba et al., 2010; Delfosse et al., 2014; Han et al., 2010; Kozlowska-Makulska et al., 2010; Y. Li et al., 2019; Z. Li et al., 2019; Mangwende et al., 2009; Niblett & Claflin, 1978; Pazhouhandeh et al., 2006; Zhuo et al., 2014) These publications conclude that each of these poleroviruses have a silencing suppressor P0 and that P0 leads to the degradation of AGO1. P0 limits the virus to the phloem of the plant along with other proteins. There are also speculations that P0 is needed for systemic movement in the plant. (Baumberger et al., 2007) However, all mechanisms found for P0 do not match across species. For example, P0 from Sugarcane yellow leaf virus targets DCL4 for degradation, but no interaction with AGO1 has been found (Mangwende et al., 2009).

Although there is evidence that the MaYMV polerovirus isolate was obtained from plants with Maize lethal necrosis symptoms, contribution to Maize lethal necrosis cannot be assumed. To confirm a causal role, direct evidence for maize infection with the clone should be established. Moreover, it will be important to establish that severe symptoms result when co-infecting maize with the MaYMV polerovirus and MCMV.

Unfortunately, the movement of virus particle across country lines is limited, and most research therefore relies on the use of infectious clones.

This study concludes that the MaYMV KARLO isolate has a P0 protein that acts as the silencing suppressor. This silencing suppressor was found to be decreasing the accumulation of virus-derived RNAs. This decrease was due to the degradation of AGO proteins. As been previously studied, this P0 lead to the degradation of AGO 1. However, P0 from the MaYMV polerovirus lead to the degradation of AGO 2, 5, 7, and 10 as well. The degradation of these AGO proteins affect the stability of virus-derived siRNA and the development of the plant. These results show that the MaYMV KARLO isolate P0 protein is a strong silencing suppressor that could be contributing to Maize lethal necrosis.

In this work we analyze the polerovirus associated to Maize lethal necrosis in Eastern Africa. Maize lethal necrosis is a complex epidemic that has needs to be critically analyzed. Understanding the individual mechanisms involved with each virus causing it is important. These observations in the mechanistic activity of P0 in the MaYMV polerovirus isolate provide informative insight into the detrimental nature of Maize lethal necrosis. We hypothesize that co-infection of multiple viruses that target different areas of the silencing suppression pathway increase severity of the symptoms. More dual virus studies are needed to understand how multiple virus infections affect plant cells.

MATERIALS AND METHODS

DNA Plasmids

Gateway entry (pENTR) and destination (pMDC32) vectors were used to make all plasmids using standard cloning techniques. The Sanger sequence-confirmed sequence was constructed in a 5’ to 3’ orientation between the 35S promoter and the nopaline synthase (NOS) terminator. The P0 sequences was synthesized from Maize yellow dwarf virus-RMV isolate KARLO, complete genome GenBank accession number MH205607.1.

pPZP-ssGFP. This vector was described in (Powers et al., 2008)

pMDC32-Empty. This vector was described in (Garcia-Ruiz et al., 2018)

pENTR-P0. pUC57-P0, synthesized by ©GENEWIZ, is a P0 ORF for MaYMV, Kenya isolate. This was inserted into pENTR by TOPO cloning using oligos 1220 and 1221 (All oligos outlined in Supplementary 1).

pMDC32-P0. pENTR-P0 was moved into pMDC32 using LR recombination.

pENTR-P0-6HIS3XFLAG. The 6HIS3xFlag tag was added to the C terminus of P0 by PCR amplification of the P0 ORF from pMDC32-P0 with oligos 1220 and 1222.

pMDC32-P0-6HIS3XFLAG. pENTR-P0-6HIS3XFLAG was moved into pMDC32 using LR recombination.

pENTR-P0-Fbox. Inactivating mutations L56V, P57A, L58I, M59L, and L60A in P0 were introduced through site-directed mutagenesis by rolling circle PCR (Qi & Scholthof, 2008) using pENTR-P0-6HIS3XFLAG as the template and oligos numbered as 1270 and 1271.

pMDC32-P0-Fbox. pENTR-P0- Fbox was moved into pMDC32 using LR recombination.

pENTR-P0-R114Q/G118L. Inactivating mutations R114Q and G118L in P0 were introduced using the same method as pENTR-P0-Fbox, but with oligos numbered as 1250 and 1251.

pMDC32-P0-R114Q/G118L. pENTR-P0- R114Q/G118L was moved into pMDC32 using LR recombination.

pENTR-P0-R2A. Inactivating mutation R2A in P0 were introduced using the same method as pENTR-P0-Fbox, but with oligos numbered as 1317 and 1318.

pMDC32-P0-R2A. pENTR-P0-R2A was moved into pMDC32 using LR recombination.

pMDC32-HC-Pro(TuMV). This vector was described in (Garcia-Ruiz et al., 2010)

pMDC32-P19-HA. This vector was described in (Garcia-Ruiz et al., 2018)

pPZP-TCV-GFP(mGC3). This vector was described in (Powers et al., 2008)

Plant materials

Wild-type *Nicotiana benthamiana* plants were and grown at 24°C under long day conditions (16 h light and 8 h dark) in University of Nebraska-Lincoln green houses. These plants were transplanted after 2 weeks of growth in autoclaved germination soil into individual 3in by 3in by 3in pots with standard soil. These individual plants grew for two more weeks before being used for experiments when they had 5 to 6 leaves showing.

Agrobacterium transformation and agroinfiltration

Agrobacterium tumefaciens strain GV3101 was transformed by electroporation as previously described (Ocampo Ocampo et al., 2016) with aforementioned pMDC32 plasmids at the C terminus. This transformation occurs by inserting the transformable strain of bacteria in a cassette with the solution of isolated DNA. When shocked, the

DNA will enter the bacteria. These bacteria are plated onto selective media and only the bacteria with the DNA with the resistant protein to the antibiotic will survive. Single-stranded green fluorescent protein (ssGFP) reporter was carried by pPZP-35S-GFP. Parental TuMV-GFP or derivatives were expressed from pCB302 plasmids (Garcia-Ruiz et al., 2010, 2015).

Using *Nicotiana benthamiana* plants in a standard assay (Johansen & Carrington, 2001) was used to measure silencing suppression of the ssGFP reporter. This standard assay using needless syringes to inject a solution of virus particles into the plant through the stomata on the underside of the leaf. A. tumefaciens cells carrying the ssGFP (OD600 = 0.25) were infiltrated in combination with P0 (OD600 = 0.5) or controls stated in the figure legend. Empty pMDC32 or beta-glucuronidase dsGUS construct (pRTL2-dsGUS) previously described by (Johansen & Carrington, 2001) were used as negative controls for the indicated experiments. Potyviral HC-Pro or tombusviral P19-HA were used as positive controls for the indicated experiments. For each treatment in any standard transient assay, 4 plants were infiltrated at leaves three and four and the experiment was repeated three times. Plants were incubated in the growth chamber at long day conditions. Ultraviolet (UV) light was shown onto the leaves in a dark room. Using a standard camera with a yellow-light filter, photographs of infiltrated leaves were taken under at 3 or 4 days post infiltration. ImageJ bundled with Java 1.8.0_172 was used to measure GFP fluorescence from the UV pictures (Garcia-Ruiz et al., 2018). At 2 to 4 days depending on the assay, the leaf tissue was collected, and protein and RNA was extracted using a glycine grinding buffer (Ocampo Ocampo et al., 2015). In Assays using Argonautes, samples were collected at 2 days post

infiltration. HA-AGO 1, HA-AGO 2, HA-AGO 4, HA-AGO 5, HA-AGO 7, HA-AGO 10 were described in (Garcia-Ruiz et al., 2015).

Western and Northern Analyses

Western blot analysis techniques were previously described (Garcia-Ruiz et al., 2018). This technique used Precision Plus Dual Color Biorad markers to read the correct size of the band. Depending on the size and saturation of the protein, the loading amount was between 2 and 10 microliter into 12% pre-made gels. Ponceau S was used to stain the membrane. Membranes were blocked in a 5% milk PBST solution. Anti-flag, anti-GFP, anti-HSP70, and Inti-rabbit IgG (GE Healthcare Na934-1) were used to probe for proteins.

Northern blot analysis techniques were as previously described (Garcia-Ruiz et al., 2010; Ocampo Ocampo et al., 2016). Urea gels were made in-lab as 17% PAGE UREA small RNA gels. RNA dye was added in equal parts to the RNA sample. Gels were transferred to a Nylon Membrane, Positively Charged (Roche # 11 417 240 001). The membrane was crosslinked twice to stabilize the RNA to the membrane. Perfect Hyb Plus Hybridization Buffer and Northern Max Prehyb/Hyb buffer was used to coat the membrane. Prehybridzation and hybridization temperatures were set to the specific RNA being probed for. Anti-Digoxigenin-AP Fab Fragments antibody was used to block the membrane. CDP-Star Ready was used to visualize the RNA in the BioRad Chemiluminescence machine.

Statistical Analyses

All measurements taken by ImageJ were averaged over all experiments. The negative control group was always used to normalize all data. Error bars represent the standard deviation across the mean of all samples.

CHAPTER 4

P0 DOES NOT AFFECT siRNA PRODUCTION

AND

P0 IS DEGRADED BY AGO PROTEINS WHEN P0 CONENTRATIONS ARE LOW

Holste, N. and Garcia-Ruiz, H.

INTRODUCTION

RNA silencing is a sequence-specific mechanism for gene inactivation. It has a variety of functions ranging from controlling gene expression (Matzke et al., 2004) to regulating viral infection in plants, insects, and invertebrates (Ding and Voinnet, 2007). RNA silencing is facilitated by 21-24nt double-stranded RNA (dsRNA) molecules that target mRNA molecules in a sequence-specific manner and can regulate gene expression on the transcriptional, post-transcriptional, and translational levels. Two types of RNA that are important for RNA interference include short interfering RNAs (siRNAs) and microRNAs (miRNAs) (Hammond, 2005).

As with other organisms, the RNA silencing pathway in plants is triggered by the presence of double-stranded RNAs (dsRNAs). The dsRNAs are processed by DICER-like enzymes that have dsRNA-specific endonucleases. (Jaskiewicz & Filipowicz, 2008) Virus-derived small interfering RNAs (vsiRNAs) originate from this process. Argonaute (AGO) proteins recruit small RNA molecules to perform antiviral functions. (Höck & Meister, 2008; Vaucheret, 2008) AGO proteins target vsiRNAs from the genomic and sub-genomic viral transcripts for degradation. (Ding & Voinnet, 2007). The Arabidopsis genome encodes 10 AGO family proteins with AGO1, AGO2, AGO5, AGO7, and AGO10 showing signs of antiviral activity within the RNA-induced silencing complex (RISC). However, the most studied of this AGO family is AGO1 where most AGO protein predictions are made from. (N. Baumberger & Baulcombe, 2005; Mi et al., 2008; Qi et al., 2005; Qu et al., 2008; Takeda et al., 2008)

Suppressor proteins are used to counteract antiviral silencing. These proteins have several methods of RNA silencing suppression: siRNA sequestration, dsRNA-binding or inhibition, and host protein contact. (Deleris et al., 2006; Glick et al., 2008;

Lakatos et al., 2006; X. Zhang et al., 2006) Polerovirus P0 proteins have been seen to use virus to host protein contact to interfere with the formation of RISC. (Bortolamiol et al., 2007; Li et al., 2019; Pazhouhandeh et al., 2006) It is suggested that P0 acts as an F-box protein to target AGO proteins for degradation using the S-phase kinase-related protein 1 (SKP1) degradation pathway within the SKP1-Cullin 1-F-box (SCF) E3 ubiquitin ligase complex. (Almasi et al., 2015; Li et al., 2019; Pazhouhandeh et al., 2006; Zhou & Howley, 1998)

Maize yellow mosaic virus (MaYMV) is a polerovirus. P0 protein is the RNA silencing suppressor that inhibits local and systemic RNA silencing. (Chen et al., 2016) In this chapter, we confirm previous findings that polerovirus P0 does not affect the biogenesis of vsiRNA. (Csorba et al., 2010) Furthermore, we show that P0 is degraded by AGO proteins 1, 2, 7, and 10 when P0 is at low concentrations. AGO5 was found to have variable effects on P0. These results complement previous results shown that P0 degrades AGO 1, 2, 5, 7, and 10 at when at high concentrations (Chapter 3).

MATERIALS AND METHODS

Plasmids, plant materials, Agrobacterium transformation, agroinfiltration, western blot analysis, northern blot analysis, graphical quantification used in Chapter 4 are described in Chapter 3.

Two suppressor co-infiltration assay

To understand the effect of siRNA when HC-Pro and P0 are present, TuMV and P0 were co-infiltrated. P0-HF, P0-R2A-HF, GUS, and P19 had an OD of 0.5 where TuMV-GFP and TuMV-AS9-GFP had an OD of 0.125 upon infiltration. Protein and RNA was extracted at 3dpi.

To visualize the presence of P0 and TuMV coat protein, a western blot analysis was performed. Of the protein sample obtained, 5 uL was loaded into a Bio-Rad 4–20% Mini-PROTEAN® TGX Stain-Free™ Protein Gels, 15 well, 15 µl. Anti-flag was used to probe for P0-HF and P0-R2A. Anti-TuMV CP (PVAS-134) was used to probe for the coat protein of TuMV-GFP and TuMV-AS9-GFP. HSP70 (Agrisera #AS09 592) with secondary antibody anti-rabbit IgG (GE Healthcare NA934-1) was used to probe for the loading control. The graphical representation of CP accumulation was normalized to the respective loading control, HSP70. Buffer was set to 0 and the respective P19 for each treatment was set to 1. All values in between are relative to the 0 and the 1 value represented.

To visualize the presence of TuMV-derived siRNA and GFP-derived siRNA, a northern blot analysis was performed. Of the RNA sample obtained, 15uL was loaded into the in-house-made gel. A DIG-labeled probe made by random priming of cDNA corresponding to CI probed for the presence of TuMV derived siRNA (Garcia-Ruiz et al., 2015). A GFP DIG-labeled probe was used to probe for the presence of GFP-derived siRNA. U6 was probed for as the loading control. All hybridization temperatures were set to 38°C and washing temperatures were set to 42°C. The graphical representation of CI and GFP accumulation was normalized to the respective loading control, U6. Buffer was set to 0 and the respective P19 for each treatment was set to 1. All values in between are relative to the 0 and the 1 value represented.

Dose response on p0 with ARGONAUTE 1, 2, 5, 7, and 10

To understand the effect of AGO 1, 2, 5, 7, and 10 on the presence of P0, we performed a dose response curve on P0. P0-HF was infiltrated at 4 different doses

with an OD of 0.063, 0.031, 0.016, and 0.0078 with AGO proteins all at an OD of 0.5. Protein was extracted at 2dpi.

To visualize the presence of P0 and AGO proteins, a western blot analysis was performed. For Figure 4.6a, 4uL was loaded into Bio-Rad 4–20% Mini-PROTEAN® TGX Stain-Free™ Protein Gels, 15 well, 15 µl. For Figure 4.6b, 6 uL was loaded into Bio-Rad 4–20% Mini-PROTEAN® TGX Stain-Free™ Protein Gels, 18 well, 30 µl. Anti-flag was used to probe for P0-HF and P0-R2A. Anti-HA (3F10, Roche 12-013-819-001) was used to probe for the AGO proteins because of their HA tag (Garcia-Ruiz et al., 2015). HSP70 (Agrisera #AS09 592) with secondary antibody anti-rabbit IgG (GE Healthcare NA934-1) was used to probe for the loading control. The graphical representation of Flag accumulation was normalized to the respective loading control, HSP70. Buffer and respective AGO protein plus empty vector treatment was set to 0 and the respective P0 plus empty vector treatment was set to 1. The value of the respective AGO protein plus P0 in between are relative to the 0 and the 1 value represented.

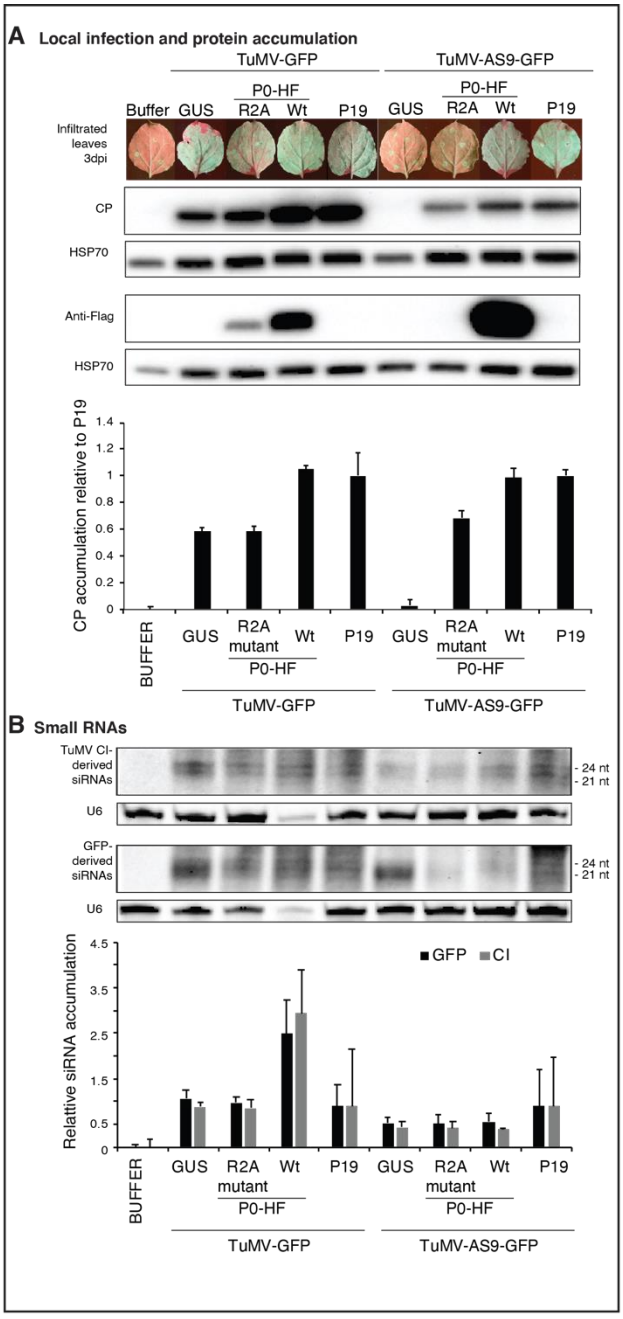

Figure 4.1. Effect of protein accumulation and vsiRNA in the presence of P0 with wild type and mutant TuMV in wild type *N. benthamiana* leaves. P0 was co-infiltrated (OD=0.5) with TuMV-GFP (OD=0.125) and P0 was co-infiltrated (OD=0.5) with TuMV-AS9-GFP (OD=0.125). The images represent the leaves with each co-infiltration at 3dpi under UV light. Protein and siRNA were extracted at 3dpi. Buffer and GUS were negative controls as described earlier. P19 was the positive control as described earlier. (A) Western blot analysis indicating that P0 assists wild type and mutant TuMV infection. The coat protein (CP) of TuMV was probed to visualize viral load in the leaves. Flag was probed for to visualize presence of P0 and P0-R2A. HSP70 was used as the loading control. The graph

quantifies the accumulation of TuMV CP. (B) Northern blot analysis indicating that P0 does not affect siRNA biogenesis. TuMV CI-derived siRNA and GFP-derived siRNA was probed for detection. The housekeeping gene, U6, was probed for as a loading control. The graph quantifies accumulation of levels of both CI and GFP- derived siRNA.

RESULTS

P0 does not inhibit vsiRNA biogenesis

We first analyzed the effect of P0 on vsiRNA production. We previously showed that GFP-derived siRNA was depleted when P0 was present (Figure 3.3). Figure 3.4 showed us that P0 effects siRNA stability by leading to the degradation of AGO proteins 1, 2, 5, 7, and 10. However, these results do not provide information about the step at which the vsiRNA is being targeted during their production. To solve if P0 is affecting the biogenesis of vsiRNA, P0 was co-infiltrated with TuMV and TuMV lacking HC-Pro, an siRNA sequestering silencing suppressor. (Garcia-Ruiz et al., 2015). Since HC-Pro binds to siRNA—ensuring siRNA stability-- P0 would still have an effect on the siRNA if it disrupts siRNA biogenesis.

Figure 4.1A shows that P0 helps increase the viral load when co-infiltrated with TuMV-GFP. This is most likely due to having two silencing suppressors—HC-Pro and P0-- that inhibit two separate parts of the RNA silencing pathway. As Figure 3.2A supported, Figure 4.1A shows us again that P0 reestablishes infection in TuMV-AS9-GFP, although not to the same level as wild type TuMV-GFP with P0.

Figure 4.1B establishes that P0 does not affect vsiRNA biogenesis. The siRNA derived from the CI protein of TuMV and siRNA from the GFP added to TuMV increases when P0 is present. This can be explained by the increase CP in Figure 4.1A when P0 is present. The positive control, P19, does not lead to an increase in vsiRNA following the pattern of CP in Figure 4.1A because P19 sequesters siRNA just like HC-Pro.

(Lakatos et al., 2006) Since siRNA is still present when HC-Pro and P0 is present as well, is not affecting siRNA production-- the step before siRNA sequestration.

P0 is degraded when present at low concentrations with AGO 1, 2, 7, and 10

In order to understand the effect of AGO proteins on P0 we performed a dose response curve on P0 co-infiltrated with constant concentrations of AGO proteins. To understand the dose that we needed to obtain clear results of the effect of AGO proteins on P0, we show the whole dose response curve of AGO1. This showed us that at concentrations of P0 with an OD of 0.0016 or lower will show what effect AGO proteins have on P0 (Figure 4.2A). AGO1 shows a dose-dependent degradation by P0. With an increase in the OD of P0, there is a decrease in the accumulation of AGO1, as expected. However, P0 is degraded by AGO1 when co-infiltrated at both 0.016 and 0.0078 OD.

To test this result on the other AGO proteins, the same dose response curve on P0 was performed on AGO 1, 2, 5, 7, and 10 at constant concentration (data not shown). All AGO proteins showed an effect on P0 at concentrations of 0.0078 (Figure 4.2B). From all AGO proteins tested, P0 is degraded by AGO 1, 2, 7, and 10. However, P0 accumulation is variable when in the presence of AGO 5.

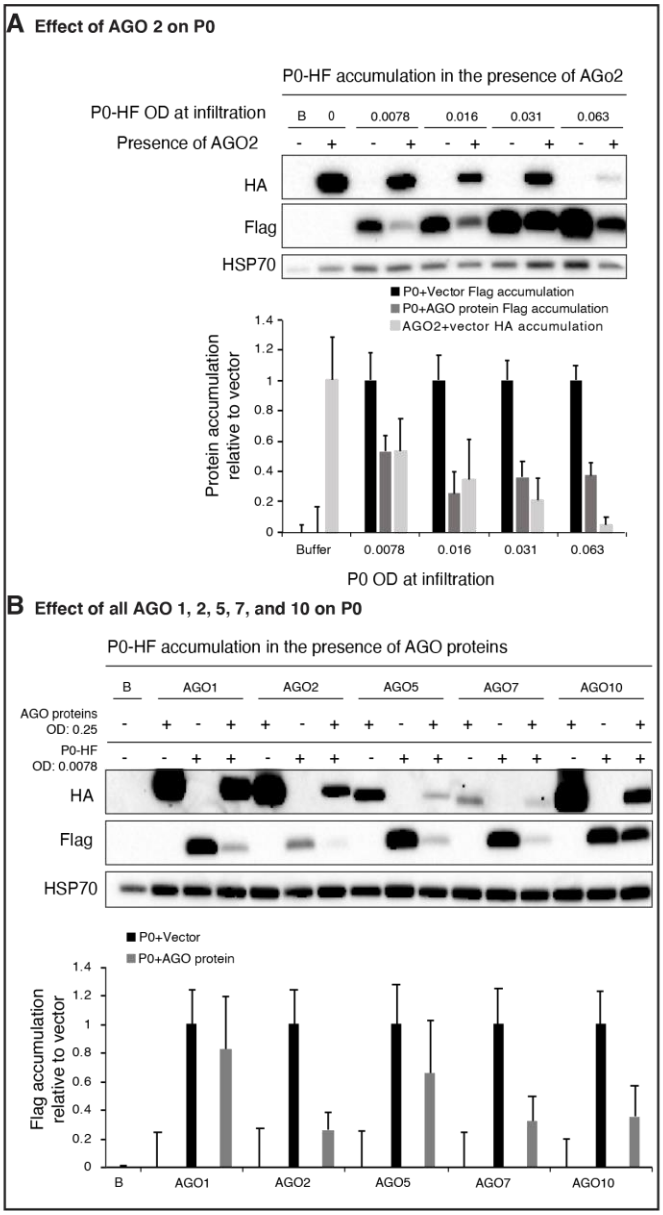

Figure 4.2. Effect of various AGOs on P0 accumulation in wild type *N. benthamiana* leaves. (A) HF-tagged P0 was co-infiltrated at OD 0.0078, 0.016, 0.031, and 0.063 with HA-tagged AGO2 at OD 0.25. Protein was extracted collected at 2 days post infiltration. The buffer solution (B), an empty vector, and an empty vector co-infiltrated with AGO2 were used as negative controls. Anti-HA probed for AGO expression while Anti-Flag probed for HF expression. HSP70 was used as a loading control. The addition of AGO2 resulted in a decrease in P0 visible when P0 was at OD of 0.016 and below. The graph quantifies the accumulation of both AGO2 and P0 protein. (B) HF-tagged P0 was co-infiltrated at OD 0.0078 with HA-tagged AGOs 1, 2, 5, 7, and 10 at OD 0.25. Protein was extracted collected at 2 days post infiltration. The buffer solution (B), an empty vector, and an empty vector co-infiltrated with all AGOs were used as negative controls. Anti-

HA probed for AGO expression while Anti-Flag probed for HF expression. HSP70 was used as a loading control. The addition of AGOs 1, 2, 5, 7, and 10 resulted in a decrease in P0. The graph quantifies the accumulation of P0 with and without AGO proteins.

DISCUSSION

Factors involved in antiviral silencing overlap the host's small rna pathways. These factors are the small RNA binding effectors, AGO proteins, and small RNA biogenesis and its components. (Garcia-Ruiz et al., 2015) AGO 1, 2, 5, 7, and 10 have antiviral activity (Chiu et al., 2010; H. Zhang et al., 2015) AGO proteins use translation repression or slicing to repress viral RNA. All flowering plants have AGO proteins with 17 AGO proteins specifically in maize. (H. Zhang et al., 2015)

AGO proteins are essential for plant development. AGO 1 is the most studied AGO protein and is known to mediate miRNA regulation for development and stress responses. (Rogers & Chen, 2013)AGO 2 associates with miRNAs with high levels of adenosine and binds miRNA and vsiRNA. Maize has two homologs of AGO2 named AGO2a and AGO2b. (Pumplin & Voinnet, 2013) Garcia-Ruiz et. al. (2015) shows that AGO2 plays a major antiviral role and interacts with vsiRNA more so than AGO1 does. It is suggested that in the event AGO1 is not working, AGO2 is able to compensate for the lack of function. AGO 5 is expressed in somatic cells and mother cells within megaspores. Maize carries three homologs of AGO5 named AGO5a, AGO5b, and AGO5c. (Tucker et al., 2012) AGO 7 has been found to bind miRNA390 and generate trans-acting siRNA. (Douglas et al., 2010) AGO10 regulates shoot apical meristems by preventing sequestering miRNA 165 and miRNA 166 which simultaneously prevents the same miRNAs from loading onto AGO1. Two homologs of AGO10 were found in maize

as well. (Qian et al., 2011) AGO10 was found to interact with vsiRNA more than AGO1 as well. (Garcia-Ruiz et al., 2015)

P0 is known to target an essential step for early development. In Arabidopsis thaliana, P0 created abnormal phyllotaxy and reduced fertility with symptoms increasing with increasing P0. (Bortolamiol et al., 2007; Csorba et al., 2010) Previous work has suggested P0 could be targeting other AGO proteins. (Bortolamiol et al., 2007) We show in chapter 3 (Figure 3.4) that P0 did lead to the degradation of AGO 1, 2, 5, 7, and 10. As stated, these AGO proteins are all important for plant development, essential, functions, and participates in antiviral activity. However, P0 does not directly interact with AGO proteins. (Bortolamiol et al., 2007; Li et al., 2019)

When P0 is present, polyubiquitination in the plant increases 10-fold more than if HC-Pro is present. (Csorba et al., 2010) This is due to P0 leading to the degradation of AGO1, 2 ,5, 7, and 10 (Figure 3.4). P0 interacts with the SKP1 using the F-box-like motif. After modifications are made downstream, the SCF-P0 complex is formed. (Li et al., 2019) SCF-P0 complex targets AGO1 and leads to its degradation in a proteasome-independent manner. (Csorba et al., 2010; Li et al., 2019) When P0 is not coupled with SKP1, it becomes instable and is degraded. At low doses, this degradation can be detected occurring with AGO 1, 2, 7, and 10 (Figure 4.2). The variability of the effect on P0 by AGO5 can possibly be explained by the multiple AGO5 homologs that exist in maize.

siRNA sequestration is the most common silencing suppression mechanism (Csorba et al., 2010). A major connection Garcia-Ruiz et. al. (2015) made was that HC-Pro inhibits siRNA loading onto AGO proteins using this process. P0 shows no signs of

RNA binding and it does not affect RISC once it is formed. (Csorba et al., 2010) Combining both P0 and HC-Pro in one infiltration showed us that HC-Pro effects the siRNA before P0 does (Figure 4.1B). As for the P0-R2A mutant, HC-Pro disrupts silencing and then protects the P0-R2A mutant from degradation (Figure 4.1A), similar to Csorba et. al. (2010). An increase in viral coat protein when both P0 and HC-Pro are present indicate a synergistic capability of having P0 coupled with a silencing suppressor of a different function. Because of the widespread distribution of P0 within the poleroviruses and enamoviruses across hosts and countries, there is much potential for co-infections. Because of the limitation to phloem in poleroviruses, a second virus suppressing silencing in non-phloem areas allow for an increased robustness in poleroviruses. (Baumberger et al., 2007) This allows for more severe diseases. Couple this with a virus that targets another aspect of the RNA silencing pathway different from P0, and the viral symptoms can only be predicted to worsen. Future work on this should include a better understanding the interaction of AGO4 with P0 and understanding the pathway of degradation.

REFERENCES

Adams, I. P., Miano, D. W., Kinyua, Z. M., Wangai, A., Kimani, E., Phiri, N., Reeder, R., Harju, V., Glover, R., Hany, U., Souza-Richards, R., Deb Nath, P., Nixon, T., Fox, A., Barnes, A., Smith, J., Skelton, A., Thwaites, R., Mumford, R., & Boonham, N. (2013). Use of next-generation sequencing for the identification and characterization of maize chlorotic mottle virus and sugarcane mosaic virus causing maize lethal necrosis in kenya. Plant Pathology, 62(4), 741–749. https://doi.org/10.1111/j.1365-3059.2012.02690.x

Agrofoglio, Y. C., Delfosse, V. C., Casse, M. F., Hopp, H. E., Bonacic Kresic, I., Ziegler-Graff, V., & Distéfano, A. J. (2019). P0 protein of cotton leafroll dwarf virus-atypical isolate is a weak <scp>RNA</scp> silencing suppressor and the avirulence determinant that breaks the cotton Cbd gene-based resistance. Plant Pathology, 68(6), 1059–1071. https://doi.org/10.1111/ppa.13031

Almasi, R., Miller, W. A., & Ziegler-Graff, V. (2015). Mild and severe cereal yellow dwarf viruses differ in silencing suppressor efficiency of the P0 protein. Virus Research, 208, 199–206. https://doi.org/10.1016/j.virusres.2015.06.020

Alvarado, V., & Scholthof, H. B. (2009). Plant responses against invasive nucleic acids: RNA silencing and its suppression by plant viral pathogens. In Seminars in Cell and Developmental Biology (Vol. 20, Issue 9, pp. 1032–1040). Elsevier Ltd. https://doi.org/10.1016/j.semcdb.2009.06.001

Baumberger, N., & Baulcombe, D. C. (2005). Arabidopsis ARGONAUTE1 is an RNA Slicer that selectively recruits microRNAs and short interfering RNAs. Proceedings of the National Academy of Sciences of the United States of America, 102(33), 11928–11933. https://doi.org/10.1073/pnas.0505461102

Baumberger, N., Tsai, C. H., Lie, M., Havecker, E., & Baulcombe, D. C. C. (2007). The Polerovirus Silencing Suppressor P0 Targets ARGONAUTE Proteins for Degradation. Current Biology, 17(18), 1609–1614. https://doi.org/10.1016/j.cub.2007.08.039

Bedhomme, S.; La_orgue, G.; Elena, S.F. Multihost experimental evolution of a plant RNA virus reveals local adaptation and host-specific mutations. Mol. Biol. Evol. 2012, 29, 1481–1492.

Bologna, N. G., & Voinnet, O. (2014). The Diversity, Biogenesis, and Activities of Endogenous Silencing Small RNAs in Arabidopsis . Annual Review of Plant Biology, 65(1), 473–503. https://doi.org/10.1146/annurev-arplant-050213-035728

Bortolamiol, D., Pazhouhandeh, M., Marrocco, K., Genschik, P., & Ziegler-Graff, V. (2007). The Polerovirus F Box Protein P0 Targets ARGONAUTE1 to Suppress RNA Silencing. Current Biology, 17(18), 1615–1621. https://doi.org/10.1016/j.cub.2007.07.061

Boulila, M. (2011). Selective constraints, molecular recombination structure and phylogenetic reconstruction of isometric plant RNA viruses of the families Luteoviridae and Tymoviridae. Biochimie, 93(2), 242–253. https://doi.org/10.1016/j.biochi.2010.09.017

Byrne, M.J., Steele, J.F.C., Hesketh, E.L., Walden, M., Thompson, R.F., Lomonossoff, G.P., and Ranson, N.A. (2019). Combining Transient Expression and Cryo-EM to

Obtain High-Resolution Structures of Luteovirid Particles. Structure 27, 1761-1770.e1763. doi: 10.1016/j.str.2019.09.010.

Cao, M., Du, P., Wang, X., Yu, Y. Q., Qiu, Y. H., Li, W., Gal-On, A., Zhou, C., Li, Y., & Ding, S. W. (2014). Virus infection triggers widespread silencing of host genes by a distinct class of endogenous siRNAs in Arabidopsis. Proceedings of the National Academy of Sciences of the United States of America, 111(40), 14613–14618. https://doi.org/10.1073/pnas.1407131111

Carbonell, A., Fahlgren, N., Garcia-Ruiz, H., Gilbert, K. B., Montgomery, T. A., Nguyen, T., Cuperus, J. T., & Carrington, J. C. (2012). Functional analysis of three Arabidopsis argonautes using slicer-defective mutants. Plant Cell, 24(9), 3613–3629. https://doi.org/10.1105/tpc.112.099945

Chen, S., Jiang, G., Wu, J., Liu, Y., Qian, Y., & Zhou, X. (2016). Characterization of a Novel Polerovirus Infecting Maize in China. Viruses, 8(5), 120. https://doi.org/10.3390/v8050120

Chiu, M. H., Chen, I. H., Baulcombe, D. C., & Tsai, C. H. (2010). The silencing suppressor P25 of Potato virus X interacts with Argonaute1 and mediates its degradation through the proteasome pathway. Molecular Plant Pathology, 11(5), 641–649. https://doi.org/10.1111/j.1364-3703.2010.00634.x

Csorba, T., Lózsa, R., Hutvágner, G., & Burgyán, J. (2010). Polerovirus protein P0 prevents the assembly of small RNA-containing RISC complexes and leads to degradation of ARGONAUTE1. Plant Journal, 62(3), 463–472. https://doi.org/10.1111/j.1365-313X.2010.04163.x

Dawson, N., Martin, A., & Sikor, T. (2016). Green Revolution in Sub-Saharan Africa: Implications of Imposed Innovation for the Wellbeing of Rural Smallholders. World Development, 78, 204–218. https://doi.org/10.1016/j.worlddev.2015.10.008

DeBlasio SL, Xu Y, Johnson RS, Rebelo AR, MacCoss MJ, Gray SM, Heck M. 2018. The interaction dynamics of two Potato leafroll virus movement proteins affects their localization to the outer membranes of mitochondria and plastids. Viruses 10. doi: 10.3390/v10110585.

DeBlasio, S. L., Chavez, J. D., Alexander, M. M., Ramsey, J., Eng, J. K., Mahoney, J., Gray, S.M., Bruce, J.E., and Cilia, M. 2015. Visualization of host-polerovirus interaction topologies using protein interaction reporter technology. Journal of Virology, 90(4), 1973-1987. doi:10.1128/JVI.01706-15.

Deleris, A., Gallago-Bartolome, J., Bao, J., Kasschau, K. D., Carrington, J. C., & Voinnet, O. (2006). Hierarchical action and inhibition of plant dicer-like proteins in antiviral defense. Science, 313(5783), 68–71. https://doi.org/10.1126/science.1128214

Delfosse, V. C., Agrofoglio, Y. C., Casse, M. F., Kresic, I. B., Hopp, H. E., Ziegler-Graff, V., & Distéfano, A. J. (2014). The P0 protein encoded by cotton leafroll dwarf virus (CLRDV) inhibits local but not systemic RNA silencing. Virus Research, 180, 70–75. https://doi.org/10.1016/j.virusres.2013.12.018

Ding, S. W., & Voinnet, O. (2007). Antiviral Immunity Directed by Small RNAs. In Cell (Vol. 130, Issue 3, pp. 413–426). NIH Public Access. https://doi.org/10.1016/j.cell.2007.07.039

Dombrovsky, A., Glanz, E., Lachman, O., Sela, N., Doron-Faigenboim, A., & Antignus, Y. (2013). The Complete Genomic Sequence of Pepper Yellow Leaf Curl Virus (PYLCV) and Its Implications for Our Understanding of Evolution Dynamics in the Genus Polerovirus. PLoS ONE, 8(7), e70722. https://doi.org/10.1371/journal.pone.0070722

Donaire, L., Wang, Y., Gonzalez-Ibeas, D., Mayer, K. F., Aranda, M. A., & Llave, C. (2009). Deep-sequencing of plant viral small RNAs reveals effective and widespread targeting of viral genomes. Virology, 392(2), 203–214. https://doi.org/10.1016/j.virol.2009.07.005

Douglas, R. N., Wiley, D., Sarkar, A., Springer, N., Timmermans, M. C. P., & Scanlon, M. J. (2010). Ragged seedling2 encodes an ARGONAUTE7-like protein required for mediolateral expansion, but not dorsiventrality, of maize leaves. Plant Cell, 22(5), 1441–1451. https://doi.org/10.1105/tpc.109.071613

Frankema, E. (2014). Africa and the green revolution a global historical perspective. NJAS - Wageningen Journal of Life Sciences, 70, 17–24. https://doi.org/10.1016/j.njas.2014.01.003

Fukuzawa, N., Itchoda, N., Ishihara, T., Goto, K., Masuta, C., & Matsumura, T. (2010). HC-Pro, a potyvirus RNA silencing suppressor, cancels cycling of Cucumber mosaic virus in Nicotiana benthamiana plants. Virus Genes, 40(3), 440–446. https://doi.org/10.1007/s11262-010-0460-0

Fusaro, A. F., Barton, D. A., Nakasugi, K., Jackson, C., Kalischuk, M. L., Kawchuk, L. M., Vaslin, M. F. S., Correa, R. L., & Waterhouse, P. M. (2017). The luteovirus p4 movement protein is a suppressor of systemic rna silencing. Viruses, 9(10). https://doi.org/10.3390/v9100294

Garcia-Arenal, F., Fraile, A., Malpica, J. M. (2001). Variability and genetic structure of plant virus populations. Annu. Rev. Phytopathol. 39 (1), 157–186. doi: 10.1146/annurev.phyto.39.1.157

Garcia-Ruiz, H., Carbonell, A., Hoyer, J. S., Fahlgren, N., Gilbert, K. B., Takeda, A., Giampetruzzi, A., Garcia Ruiz, M. T., McGinn, M. G., Lowery, N., Martinez Baladejo, M. T., & Carrington, J. C. (2015). Roles and Programming of Arabidopsis ARGONAUTE Proteins during Turnip Mosaic Virus Infection. PLoS Pathogens, 11(3), 1–27. https://doi.org/10.1371/journal.ppat.1004755

Garcia-Ruiz, H., Gabriel Peralta, S. M., & Harte-Maxwell, P. A. (2018). Tomato spotted wilt virus NSs protein supports infection and systemic movement of a potyvirus and is a symptom determinant. Viruses, 10(3). https://doi.org/10.3390/v10030129

Garcia-Ruiz, H., Holste, N. M., & LaTourrette, K. (2020). Poleroviruses (Luteoviridae). In Reference Module in Life Sciences. Elsevier. https://doi.org/10.1016/b978-0-12-809633-8.21343-5

Garcia-Ruiz, H., Takeda, A., Chapman, E. J., Sullivan, C. M., Fahlgren, N., Brempelis, K. J., & Carrington, J. C. (2010). Arabidopsis RNA-dependent RNA polymerases and dicer-like proteins in antiviral defense and small interfering RNA biogenesis during Turnip mosaic virus infection. Plant Cell, 22(2), 481–496. https://doi.org/10.1105/tpc.109.073056

Gasciolli, V., Mallory, A. C., Bartel, D. P., & Vaucheret, H. (2005). Partially redundant functions of arabidopsis DICER-like enzymes and a role for DCL4 in producing

trans-Acting siRNAs. Current Biology, 15(16), 1494–1500. https://doi.org/10.1016/j.cub.2005.07.024

Glick, E., Zrachya, A., Levy, Y., Mett, A., Gidoni, D., Belausov, E., Citovsky, V., & Gafni, Y. (2008). Interaction with host SGS3 is required for suppression of RNA silencing by tomato yellow leaf curl virus V2 protein. Proceedings of the National Academy of Sciences of the United States of America, 105(1), 157–161. https://doi.org/10.1073/pnas.0709036105

Gray, S. M. (2008). Aphid transmission of plant viruses. In Current Protocols in Microbiology: Vol. Chapter 16 (Issue SUPPL. 10). Curr Protoc Microbiol. https://doi.org/10.1002/9780471729259.mc16b01s10

Gray, S., Cilia, M., & Ghanim, M. (2014). Circulative, non-propagative virus transmission: an orchestra of virus-, insect-, and plant-derived instruments. Advances in Virus Research (Vol. 89, pp. 141-199):

Hammond, S. M. (2005). Dicing and slicing: The core machinery of the RNA interference pathway. In FEBS Letters (Vol. 579, Issue 26, pp. 5822–5829). No longer published by Elsevier. https://doi.org/10.1016/j.febslet.2005.08.079

Han, Y. H., Xiang, H. Y., Wang, Q., Li, Y. Y., Wu, W. Q., Han, C. G., Li, D. W., & Yu, J. L. (2010). Ring structure amino acids affect the suppressor activity of melon aphid-borne yellows virus P0 protein. Virology, 406(1), 21–27. https://doi.org/10.1016/j.virol.2010.06.045

Harvey, J. J. W., Lewsey, M. G., Patel, K., Westwood, J., Heimstädt, S., Carr, J. P., & Baulcombe, D. C. (2011). An Antiviral Defense Role of AGO2 in Plants. PLoS ONE, 6(1), e14639. https://doi.org/10.1371/journal.pone.0014639

Hazra, A. (2017). Using the confidence interval confidently. J. thoracic Dis. 9 (10), 4125–4130. doi: 10.21037/jtd.2017.09.14

Höck, J., & Meister, G. (2008). The Argonaute protein family. In Genome Biology (Vol. 9, Issue 2, p. 210). BioMed Central. https://doi.org/10.1186/gb-2008-9-2-210

Huang LF, Naylor M, Pallett DW, Reeves J, Cooper JI, Wang H, 2005. The complete genome sequence, organization and affinities of carrot red leaf virus. Archives of Virology150, 1845–55.

Jaskiewicz, L., & Filipowicz, W. (2008). Role of Dicer in posttranscriptional RNA silencing. In Current Topics in Microbiology and Immunology (Vol. 320, pp. 77–97). Springer, Berlin, Heidelberg. https://doi.org/10.1007/978-3-540-75157-1_4

Johansen, L. K., & Carrington, J. C. (2001). Silencing on the spot. Induction and suppression of RNA silencing in the Agrobacterium-mediated transient expression system. In Plant Physiology (Vol. 126, Issue 3). https://doi.org/10.1104/pp.126.3.930

Kasschau, K. D., & Carrington, J. C. (2001). Long-distance movement and replication maintenance functions correlate with silencing suppression activity of potyviral HC-Pro. Virology, 285(1), 71–81. https://doi.org/10.1006/viro.2001.0901

Knierim, D., Deng, T.C., Tsai, W.S., Green, S.K., Kenyon, L. 2010. Molecular identification of three distinct polerovirus species and a recombinant Cucurbit aphid-borne yellows virus strain infecting cucurbit crops in Taiwan. Plant Pathology 59:991-1002.

Kozlowska-Makulska, A., Guilley, H., Szyndel, M. S., Beuve, M., Lemaire, O., Herrbach, E., & Bouzoubaa, S. (2010). P0 proteins of European beet-infecting

poleroviruses display variable RNA silencing suppression activity. Journal of General Virology, 91(4), 1082–1091. https://doi.org/10.1099/vir.0.016360-0

Krueger, E. N., Beckett, R. J., Gray, S. M., & Allen Miller, W. (2013). The complete nucleotide sequence of the genome of Barley yellow dwarf virus-RMV reveals it to be a new Polerovirus distantly related to other yellow dwarf viruses. Frontiers in Microbiology, 4(JUL), 205. https://doi.org/10.3389/fmicb.2013.00205

Lakatos, L., Csorba, T., Pantaleo, V., Chapman, E. J., Carrington, J. C., Liu, Y. P., Dolja, V. V., Calvino, L. F., López-Moya, J. J., & Burgyán, J. (2006). Small RNA binding is a common strategy to suppress RNA silencing by several viral suppressors. EMBO Journal, 25(12), 2768–2780. https://doi.org/10.1038/sj.emboj.7601164

Lapierre, H., Signoret, P. A., & Institut national de la recherche agronomique (France). (2004). Viruses and virus diseases of Poaceae (Gramineae). Institut national de la recherche agronomique.

Lee, L., Palukaitis, P., Gray, S.M. 2002. Host-dependent requirement for the Potato leafroll virus 17-kda protein in virus movement. Mol Plant Microbe Interact, 15, 1086-1094. doi: 10.1094/MPMI.2002.15.10.1086.

Li, Y., Sun, Q., Zhao, T., Xiang, H., Zhang, X., Wu, Z., Zhou, C., Zhang, X., Wang, Y., Zhang, Y., Wang, X., Li, D., Yu, J., Dinesh-Kumar, S. P., & Han, C. (2019). Interaction between Brassica yellows virus silencing suppressor P0 and plant SKP1 facilitates stability of P0 in vivo against degradation by proteasome and autophagy pathways. New Phytologist, 222(3), 1458–1473. https://doi.org/10.1111/nph.15702

Li, Y., Xiong, R., Bernards, M., Wang, A. (2016). Recruitment of Arabidopsis RNA helicase AtRH9 to the viral replication complex by viral replicase to promote turnip mosaic virus replication. Sci. Rep. 6, 30297. doi: 10.1038/srep30297

Liu, F., Wang, X., Liu, Y., Xie, J., Gray, S. M., Zhou, G., & Gao, B. (2007). A Chinese isolate of barley yellow dwarf virus-PAV represents a third distinct species within the PAV serotype. Archives of Virology, 152(7), 1365–1373. https://doi.org/10.1007/s00705-007-0947-8

Liu, Y., Sun, B., Wang, X., Zheng, C., & Zhou, G. (2007). Three digoxigenin-labeled cDNA probes for specific detection of the natural population of Barley yellow dwarf viruses in China by dot-blot hybridization. Journal of Virological Methods, 145(1), 22–29. https://doi.org/10.1016/j.jviromet.2007.05.006

lsevier.Kaplan, I. B., Lee, L., Ripoll, D. R., Palukaitis, P., Gildow, F., & Gray, S. M. 2007. Point mutations in the Potato leafroll virus major capsid protein alter virion stability and aphid transmission. Journal of General Virology, 88(6), 1821-1830.

Mahuku, G., Lockhart, B. E., Wanjala, B., Jones, M. W., Kimunye, J. N., Stewart, L. R., Cassone, B. J., Sevgan, S., Nyasani, J. O., Kusia, E., Kumar, P. L., Niblett, C. L., Kiggundu, A., Asea, G., Pappu, H. R., Wangai, A., Prasanna, B. M., & Redinbaugh, M. G. (2015). Maize lethal necrosis (MLN), an emerging threat to maize-based food security in sub-Saharan Africa. Phytopathology, 105(7), 956–965. https://doi.org/10.1094/PHYTO-12-14-0367-FI

Mangwende, T., Wang, M. L., Borth, W., Hu, J., Moore, P. H., Mirkov, T. E., & Albert, H. H. (2009). The P0 gene of Sugarcane yellow leaf virus encodes an RNA

silencing suppressor with unique activities. Virology, 384(1), 38–50. https://doi.org/10.1016/j.virol.2008.10.034

Massawe, D.P., Stewart, L.R., Kamatenesi, J., Asiimwe, T., Redinbaugh, M.G. 2018. Complete sequence and diversity of a maize-associated polerovirus in East Africa. Virus Genes 54:432-437. doi: 10.1007/s11262-018-1560-5.

Matzke, M., Aufsatz, W., Kanno, T., Daxinger, L., Papp, I., Mette, M. F., & Matzke, A. J. M. (2004). Genetic analysis of RNA-mediated transcriptional gene silencing. In Biochimica et Biophysica Acta - Gene Structure and Expression (Vol. 1677, Issues 1–3, pp. 129–141). Elsevier. https://doi.org/10.1016/j.bbaexp.2003.10.015

Mi, S., Cai, T., Hu, Y., Chen, Y., Hodges, E., Ni, F., Wu, L., Li, S., Zhou, H., Long, C., Chen, S., Hannon, G. J., & Qi, Y. (2008). Sorting of Small RNAs into Arabidopsis Argonaute Complexes Is Directed by the 5′ Terminal Nucleotide. Cell, 133(1), 116–127. https://doi.org/10.1016/j.cell.2008.02.034

Miller W. A., Dinesh-Kumar S. P., Paul C. P. (1995). Luteovirus gene expression. Crit. Rev. Plant Sci. 14, 179–211. 10.1080/07352689509701926

Mizianty, M. J., Stach, W., Chen, K., Kedarisetti, K. D., Disfani, F. M., & Kurgan, L. (2011). Improved sequence-based prediction of disordered regions with multilayer fusion of multiple information sources. Bioinformatics, 27(13), i489–i496. https://doi.org/10.1093/bioinformatics/btq373

Moonan F, Molina J, Mirkov TE, 2000. Sugarcane Yellow Leaf Virus: an emerging virus that has evolved by recombination between luteoviral and poleroviral ancestors. Virology269, 156–71.

Murrell, B., Wertheim, J. O., Moola, S., Weighill, T., Scheffler, K., & Kosakovsky Pond, S. L. (2012). Detecting individual sites subject to episodic diversifying selection. PLoS Genetics, 8(7), 1002764. https://doi.org/10.1371/journal.pgen.1002764

Niblett, C. L., & Claflin, L. E. (1978). Corn lethal necrosis - a new virus disease of corn in Kansas. Plant Disease Reporter, 62(1), 15–19.

Nigam, D., & Garcia-Ruiz, H. (2020). Variation profile of the orthotospovirus genome. Pathogens, 9(7), 1–28. https://doi.org/10.3390/pathogens9070521

Nigam, D., LaTourrette, K., Souza, P. F. N., & Garcia-Ruiz, H. (2019). Genome-Wide Variation in Potyviruses. Frontiers in Plant Science, 10, 1439. https://doi.org/10.3389/fpls.2019.01439

Nixon P. L., Rangan A., Kim Y. G., Rich A., Hoffman D. W., Hennig M., et al. . (2002). Solution structure of a Luteoviral P1-P2 frameshifting mRNA pseudoknot. J. Mol. Biol. 322, 621–633. 10.1016/S0022-2836(02)00779-9

Ocampo Ocampo, T., Gabriel Peralta, S. M., Bacheller, N., Uiterwaal, S., Knapp, A., Hennen, A., Ochoa-Martinez, D. L., & Garcia-Ruiz, H. (2016). Antiviral RNA silencing suppression activity of Tomato spotted wilt virus NSs protein. Genetics and Molecular Research, 15(2). https://doi.org/10.4238/gmr.15028625

Osman, T. A. M., Coutts, R. H. A., & Buck, K. W. (2006). In Vitro Synthesis of Minus-Strand RNA by an Isolated Cereal Yellow Dwarf Virus RNA-Dependent RNA Polymerase Requires VPg and a Stem-Loop Structure at the 3′ End of the Virus RNA. Journal of Virology, 80(21), 10743–10751. https://doi.org/10.1128/jvi.01050-06

Pagán, I., & Holmes, E. C. (2010). Long-Term Evolution of the Luteoviridae: Time Scale and Mode of Virus Speciation. Journal of Virology, 84(12), 6177–6187. https://doi.org/10.1128/jvi.02160-09

Patton, M. F., Bak, A., Sayre, J. M., Heck, M. L., & Casteel, C. L. (2020). A polerovirus, Potato leafroll virus, alters plant–vector interactions using three viral proteins. Plant, Cell & Environment, 43(2), 387–399. https://doi.org/10.1111/pce.13684

Pazhouhandeh, M., Dieterle, M., Marrocco, K., Lechner, E., Berry, B., Brault, V., Hemmer, O., Kretsch, T., Richards, K. E., Genschik, P., & Ziegler-Graff, V. (2006). F-box-like domain in the polerovirus protein P0 is required for silencing suppressor function. Proceedings of the National Academy of Sciences of the United States of America, 103(6), 1994–1999. https://doi.org/10.1073/pnas.0510784103

Peter, K.A., Liang, D., Palukaitis, P., Gray, S.M. 2008. Small deletions in the Potato leafroll virus readthrough protein affect particle morphology, aphid transmission, virus movement and accumulation. J Gen Virol, 89, 2037-2045. doi: 10.1099/vir.0.83625-0.

Powers, J. G., Sit, T. L., Qu, F., Morris, T. J., Kim, K. H., & Lommel, S. A. (2008). A versatile assay for the identification of RNA silencing suppressors based on complementation of viral movement. Molecular Plant-Microbe Interactions, 21(7), 879–890. https://doi.org/10.1094/MPMI-21-7-0879

Prüfer D., Tacke E., Schmitz J., Kull B., Kaufmann A., Rohde W. (1992). Ribosomal frameshifting in plants: a novel signal directs the -1 frameshift in the synthesis of the putative viral replicase of potato leafroll luteovirus. EMBO J. 11, 1111–1117.

Pumplin, N., & Voinnet, O. (2013). RNA silencing suppression by plant pathogens: Defence, counter-defence and counter-counter-defence. In Nature Reviews Microbiology (Vol. 11, Issue 11, pp. 745–760). Nature Publishing Group. https://doi.org/10.1038/nrmicro3120

Qi, D., & Scholthof, K. B. G. (2008). A one-step PCR-based method for rapid and efficient site-directed fragment deletion, insertion, and substitution mutagenesis. Journal of Virological Methods, 149(1), 85–90. https://doi.org/10.1016/j.jviromet.2008.01.002

Qi, X., Bao, F. S., & Xie, Z. (2009). Small RNA deep sequencing reveals role for Arabidopsis thaliana RNA-dependent RNA polymerases in viral siRNA biogenesis. PLoS ONE, 4(3), e4971. https://doi.org/10.1371/journal.pone.0004971

Qi, Y., Denli, A. M., & Hannon, G. J. (2005). Biochemical specialization within Arabidopsis RNA silencing pathways. Molecular Cell, 19(3), 421–428. https://doi.org/10.1016/j.molcel.2005.06.014

Qian, Y., Cheng, Y., Cheng, X., Jiang, H., Zhu, S., & Cheng, B. (2011). Identification and characterization of Dicer-like, Argonaute and RNA-dependent RNA polymerase gene families in maize. Plant Cell Reports, 30(7), 1347–1363. https://doi.org/10.1007/s00299-011-1046-6

Qu, F., Ye, X., & Morris, T. J. (2008). Arabidopsis DRB4, AGO1, AGO7, and RDR6 participate in a DCL4-initiated antiviral RNA silencing pathway negatively regulated by DCL1. Proceedings of the National Academy of Sciences of the

United States of America, 105(38), 14732–14737. https://doi.org/10.1073/pnas.0805760105

Rambaut, A. (2009). FigTree. http://tree.bio.ed.ac.uk/software/figtree. version 1.3.1. Available from: . Accessed 13 January 2015.

Rashid, M.-O., Zhang, X.-Y., Wang, Y., Li, D.-W., Yu, J.-L., and Han, C.-G. 2019. The three essential motifs in P0 for suppression of RNA silencing activity of Potato leafroll virus are required for virus systemic infection. Viruses, 11(2), 170. doi: 10.3390/v11020170.

Ritz, J.; Martin, J.S.; Laederach, A. Evolutionary evidence for alternative structure in RNA sequenceco-variation.PLoS Comput. Biol.2013, 9, e1003152

Rodamilans, B., Shan, H., Pasin, F., & García, J. A. (2018). Plant viral proteases: Beyond the role of peptide cutters. In Frontiers in Plant Science (Vol. 9, p. 666). Frontiers Media S.A. https://doi.org/10.3389/fpls.2018.00666

Rogers, K., & Chen, X. (2013). Biogenesis, turnover, and mode of action of plant microRNAs. In Plant Cell (Vol. 25, Issue 7, pp. 2383–2399). Plant Cell. https://doi.org/10.1105/tpc.113.113159

Schuck, J., Gursinsky, T., Pantaleo, V., Burgyán, J., & Behrens, S.-E. (2013). AGO/RISC-mediated antiviral RNA silencing in a plant in vitro system. Nucleic Acids Research, 41(9), 5090–5103. https://doi.org/10.1093/nar/gkt193

Shen, Y., Wan, Z., Coarfa, C., Drabek, R., Chen, L., Ostrowski, E. A., et al. (2010). A SNP discovery method to assess variant allele probability from next-generation resequencing data. Genome Res. 20 (2), 273–280. doi: 10.1101/gr.096388.109

Shiferaw, B., Prasanna, B. M., Hellin, J., & Bänziger, M. (2011). Crops that feed the world 6. Past successes and future challenges to the role played by maize in global food security. In Food Security (Vol. 3, Issue 3, pp. 307–327). Springer. https://doi.org/10.1007/s12571-011-0140-5

Sibanda, O. S. (2015). Trade liberalisation and its impact on food security in Sub-Saharan Africa. International Journal of Public Law and Policy, 5(1), 92–107. https://doi.org/10.1504/IJPLAP.2015.067782

Szilágyi, A., Györffy, D., & Závodszky, P. (2008). The twilight zone between protein order and disorder. Biophysical Journal, 95(4), 1612–1626. https://doi.org/10.1529/biophysj.108.131151

Szittya, G., & Burgyán, J. (2013). RNA Interference-Mediated Intrinsic Antiviral Immunity in Plants (pp. 153–181). Springer, Berlin, Heidelberg. https://doi.org/10.1007/978-3-642-37765-5_6

Takeda, A., Iwasaki, S., Watanabe, T., Utsumi, M., & Watanabe, Y. (2008). The mechanism selecting the guide strand from small RNA duplexes is different among Argonaute proteins. Plant and Cell Physiology, 49(4), 493–500. https://doi.org/10.1093/pcp/pcn043

Tucker, M. R., Okada, T., Hu, Y., Scholefield, A., Taylor, J. M., & Koltunow, A. M. G. (2012). Somatic small RNA pathways promote the mitotic events of megagametogenesis during female reproductive development in arabidopsis. Development, 139(8), 1399–1404. https://doi.org/10.1242/dev.075390

Uyemoto, J. K. (1980). Detection of Maize Chlorotic Mottle Virus Serotypes by Enzyme-Linked Immunosorbent Assay. Phytopathology, 70(4), 290. https://doi.org/10.1094/phyto-70-290

Vance, V., & Vaucheret, H. (2001). RNA silencing in plants - Defense and counterdefense. In Science (Vol. 292, Issue 5525, pp. 2277–2280). https://doi.org/10.1126/science.1061334

Vaucheret, H. (2008). Plant ARGONAUTES. In Trends in Plant Science (Vol. 13, Issue 7, pp. 350–358). Elsevier Current Trends. https://doi.org/10.1016/j.tplants.2008.04.007

Wamaitha, M. J., Nigam, D., Maina, S., Stomeo, F., Wangai, A., Njuguna, J. N., Holton, T. A., Wanjala, B. W., Wamalwa, M., Lucas, T., Djikeng, A., & Garcia-Ruiz, H. (2018). Metagenomic analysis of viruses associated with maize lethal necrosis in Kenya. Virology Journal, 15(1), 1–19. https://doi.org/10.1186/s12985-018-0999-2

Wan, J., Basu, K., Mui, J., Vali, H., Zheng, H., Laliberte, J. F. (2015). Ultrastructural characterization of turnip mosaic virus-induced cellular rearrangements reveals membrane-bound viral particles accumulating in vacuoles. J. Virol. 89 (24), 12441–12456. doi: 10.1128/JVI.02138-15

Wang, X. B., Jovel, J., Udomporn, P., Wang, Y., Wu, Q., Li, W. X., Gasciolli, V., Vaucheret, H., & Ding, S. W. (2011). The 21-nucleotide, but not 22-nucleotide, viral secondary small interfering rnas direct potent antiviral defense by two cooperative argonautes in Arabidopsis thaliana. Plant Cell, 23(4), 1625–1638. https://doi.org/10.1105/tpc.110.082305

Wangai, A. W., Redinbaugh, M. G., Kinyua, Z. M., Miano, D. W., Leley, P. K., Kasina, M., Mahuku, G., Scheets, K., & Jeffers, D. (2012). First Report of Maize chlorotic mottle virus and Maize Lethal Necrosis in Kenya . Plant Disease, 96(10), 1582–1582. https://doi.org/10.1094/pdis-06-12-0576-pdn

Wintermantel, W. M. (2005). Co-infection of Beet mosaic virus with Beet yellowing viruses leads to increased symptom expression on sugar beet. Plant Disease, 89(3), 325-331. doi: 10.1094/pd-89-0325.

Xu Y, Da Silva WL, Qian Y, Gray SM. 2018. An aromatic amino acid and associated helix in the C-terminus of the Potato leafroll virus minor capsid protein regulate systemic infection and symptom expression. PLoS Pathog 14:e1007451. doi: 10.1371/journal.ppat.1007451.

Zhang, H., Xia, R., Meyers, B. C., & Walbot, V. (2015). Evolution, functions, and mysteries of plant ARGONAUTE proteins. Current Opinion in Plant Biology, 27, 84–90. https://doi.org/10.1016/j.pbi.2015.06.011

Zhang, X., Yuan, Y. R., Pei, Y., Lin, S. S., Tuschl, T., Patel, D. J., & Chua, N. H. (2006). Cucumber mosaic virus-encoded 2b suppressor inhibits Arabidopsis Argonaute1 cleavage activity to counter plant defense. Genes and Development, 20(23), 3255–3268. https://doi.org/10.1101/gad.1495506

Zhou, C.-J., Zhang, X.-Y., Liu, S.-Y., Wang, Y., Li, D.-W., Yu, J.-L., & Han, C.-G. (2017). Synergistic infection of BrYV and PEMV-2 increases the accumulations of both BrYV and BrYV-derived siRNAs in Nicotiana benthamiana. Scientific Reports, 7, 45132. doi: 10.1038/srep45132.

Zhou, P., & Howley, P. M. (1998). Ubiquitination and degradation of the substrate recognition subunits of SCF ubiquitin-protein ligases. Molecular Cell, 2(5), 571–580. https://doi.org/10.1016/S1097-2765(00)80156-2

Zhuo, T., Li, Y. Y., Xiang, H. Y., Wu, Z. Y., Wang, X. Bin, Wang, Y., Zhang, Y. L., Li, D. W., Yu, J. L., & Han, C. G. (2014). Amino acid sequence motifs essential for p0-

mediated suppression of rna silencing in an isolate of potato leafroll virus from inner mongolia. Molecular Plant-Microbe Interactions, 27(6), 515–527. https://doi.org/10.1094/MPMI-08-13-0231-R